COVALENTLY FUNCTIONALIZED MSNS AS POTENTIAL PHOTOSENSITIZING AGENTS FOR PDT

A THESIS
SUBMITTED TO THE MATERIALS SCIENCE AND NANOTECHNOLOGY
PROGRAM OF THE INSTITUTE OF ENGINEERING AND SCIENCES
OF BİLKENT UNIVERSITY
IN PARTIAL FULFILLMENT OF THE REQUIREMENTS
FOR THE DEGREE OF
MASTER OF SCIENCE

By
MERVE TÜRKŞANLI
January 2011

I certify that I have read this thesis and that in my opinion it is fully adequate, in scope and in quality, as a thesis of the degree of Master of Science.

…….

Prof. Dr. Engin U. Akkaya (Principal Advisor)

I certify that I have read this thesis and that in my opinion it is fully adequate, in scope and in quality, as a thesis of the degree of Master of Science.

…….

Assist. Prof. Dr. Mehmet Bayındır

I certify that I have read this thesis and that in my opinion it is fully adequate, in scope and in quality, as a thesis of the degree of Master of Science.

…….

Prof. Dr. Özdemir Doğan

Approved for the Institute of Engineering and Science:

…….

Prof. Dr. Levent Onural

Director of the Institute of Engineering and Science

..

ABSTRACT

COVALENTLY FUNCTIONALIZED MSNS AS POTENTIAL PHOTOSENSITIZING AGENTS FOR PDT

Merve Türkşanlı
M.S. in Materials Science and Nanotechnology
Supervisor: Prof. Dr. Engin U. Akkaya
January, 2011

Photodynamic therapy (PDT) is a novel approach for the treatment of some cancers and other non-malignant diseases. PDT aims to kill cancer tissue by the generation of singlet oxygen as a result of excitation of the photosensitizer (PS) by illuminating with a light source at a certain wavelength. Mesoporous silica nanoparticles are promising in PDT issue due to their chemical inertness, biocompatibility, low-toxicity, hydrophility and ease of surface modification. We have synthesized and characterized novel boradiazaindacene (BODIPY)-based PS that is covalently attached to the pore of mesoporous silica nanoparticles (MSNs). We have observed that near infrared absorbing photosensitizer attached MSNs successfully generate cytotoxic singlet oxygen.

Keywords: Boradiazaindacene, photodynamic therapy, photosensitizer, mesoporous silica nanoparticles, drug carrier system.

ÖZET

FOTODİNAMİK TERAPİ İÇİN POTANSİYEL FOTODUYARLAŞTIRICI NITELIĞI OLAN, KOVALENT OLARAK TÜREVLENDİRİLMİŞ MEZO GÖZENEKLİ SİLİKA NANOPARÇACIKLAR

Merve Türkşanlı
Malzeme Bilimi ve Nanoteknoloji Programı, Yüksek Lisans
Tez Yöneticisi: Prof. Dr. Engin U. Akkaya
Ocak, 2011

Fotodinamik terapi, bazı kanser ve kötü huylu olmayan hastalıkların tedavisi için geliştirilmiş yeni bir yaklaşımdır. Fotodinamik terapi, fotouyarıcının belirli bir dalga boyuna sahip ışık kaynağı tarafından uyarılmasının ardından sitotoksik singlet oksijen oluşturması ile kanserli dokunun öldürülmesini amaçlar. Mezo gözenekli silika nanoparçacıklar sahip oldukları kimyasal inertlik, biyouyumluluk, düşük toksisite, hidrofilite ve yüzey modifikasyonunun kolaylığı özellikleri sebebiyle fotodinamik terapi konusunda ümit verici bir yaklaşımdır. Bu çalışmada, yeni BODIPY temelli fotoduyarlaştırıcı sentezlendi ve karakterize edildi. Bu fotoduyarlaştırıcı, mezo gözenekli silika nanoparçacık gözeneğine kovalent olarak bağlanmıştır. Yakın kızılötesi bölgede soğuran fotoduyarlaştırıcının nanoparçacığa bağlanması sonucu başarılı bir şekilde singlet oksijen oluşturduğu gözlemlenmiştir.

Anahtar Kelimeler: Boradiazaindasen, fotodinamik terapi, fotosensitizör, mezo gözenekli silika nanoparçacık, ilaç taşıma sistemi.

Dedicated to my husband

ACKNOWLEDGEMENT

I would like to express my greatest thanks to my supervisor Prof. Dr. Engin U. Akkaya for his guidance, support, and patience during the course of this research. I am also grateful to him for showing us how a good scientist can be a brilliant person in life. I will never forget his support and personality throughout my life.

I owe a special thank to Ruslan Guliyev for his support, guidance and the experience that he shared without any hesitation.

I would like to thank to Onur Büyükçakır for his support during the course of this research.

I want to thank to our group members Bilal Kılıç, Safacan Kölemen, Yusuf Çakmak, Sündüs Erbaş Çakmak, Tuğba Özdemir, Yiğit Altay, Nisa Yeşilgül, Gizem Çeltek, Ziya Köstereli, Tuba Yaşar, Fatma Pir, Şeyma Öztürk, Seda Demirel and rest of the SCL (Supramolecular Chemistry Laboratory) members. It was wonderful to work with them.

I would like to express my special thanks to my friends Çağla Özgit, Handan Acar and Okan Öner Ekiz. They added pleasure to the time that I spent on my research.

I would like to thank UNAM (Institute of Materials Science and Nanotechnology) for their financial support.

This thesis would not have been possible without the belief and support of my family. My final and the deepest thanks go to them and my husband Burkan Kaplan. I owe them a lot.

LIST OF ABBREVIATIONS

PDT:	Photodynamic Therapy
PS:	Photosensitizer
MSN:	Mesoporous Silica Nanoparticle
PS-MSN:	Photosensitizer attached mesoporous silica nanoparticle
FDA:	Food and Drug Administration
THF:	Tetrahydrofuran
TFA:	Trifluoroacetic Acid
DPBF:	1, 3 Diphenylisobenzofuran
TEM:	Transmission Electron Microscopy
SEM:	Scanning Electron Microscopy
XRD:	X-ray Diffraction
NMR:	Nuclear Magnetic Resonance
BODIPY:	Boradiazaindacene

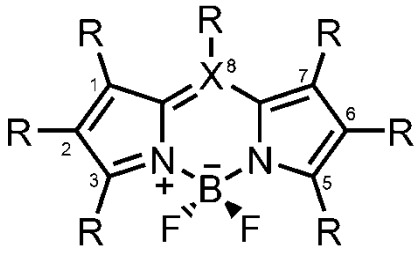

R = H or any other group
X = C or N

TABLE OF CONTENTS

LIST OF FIGURES

CHAPTER 1

INTRODUCTION

1.1 Photodynamic Therapy

Photodynamic therapy is a novel, promising approach for the treatment of some cancers and other non-malignant diseases. The therapy involves two important stages; administration of a photosensitizer and illumination of the tissue to activate the photosensitizer with the light of a specific wavelength. When the tissue is illuminated, the photosensitizer which previously localized at the tumor is excited. The excitation of the molecule leads to several molecular energy transfers and finally highly reactive and cytotoxic oxygen species called singlet oxygen ($^1O_2$) is produced [1]. In biological systems, $^1O_2$ has a lifetime of <0,04 microsecond [2]. During this very short interval, $^1O_2$ species causes cancer cells damaged or destroyed either targeting the cells directly, causing necrosis and/or apoptosis[3] or by targeting tumour or healthy surrounding vasculature [4].

PDT has numerous advantages over the traditional treatment methods of cancer such as surgery, radiotherapy and chemotherapy. Firstly, targeting is achieved by the delivery of the light. At a certain time after the administration of the drug, light is targeted into the tumour and surrounding vasculatory by fiber optic systems and endoscopy. This in turn, causes only damage of tumours. Since the life time of $^1O_2$

species is very short, it migrates less than 0.02 μm after its generation[5] . As a result it is deactivated before it can flee out of the cell.

Secondly, the tumours have abnormal physiology such as; leaks at vasculatory, lower pH value, higher number of low density protein receptors, presence of macrophages, larger amount of lipids[2]. The photosensitizers which are developed for these environments achieve selectivity. On the other hand, limitation of PDT rises because of the fact that it cannot treat the advanced disseminated diseases since the illumination of the entire body and the uptaken of the appropriate doses of drug is impossible.

As a result, for localized tumours or the early stages of the disease, PDT is a selective and usefull therapy with many advantages and for the advanced level of the disease, it improves the life quality and improves survival time.

1.1.1 History of Photodynamic Therapy

Light has been used as a therapeutic agent since ancient ages. However, in medicine and surgery, it is being used just with the beginning of the last century. Ancient Egypt, China and India took the advantage of light to treat some skin diseases, such as psoriasis, vitiligo and cancer [6]. In ancient Greek, the whole body was exposed to sunlight to treat diseases. This way of therapy was called as *heliotherapy* by the famous Greek physician Heredotus[7]. Danish physician Niels Finsen used UV light and carbon arc phototherapy for the treatment of cutaneous tuberculosis. With that study, Finsen got Nobel Prize in 1903 [7,8].

The use of light as a therapy is called as phototherapy, on the other hand, in addition to phototherapy when the photosensitizers are used, the treatment way is

called photochemotherapy. Photochemotherapy also has a history of 3000 years. Indians first employed psoralens with light to treat vitiligo [9].

Photodynamic therapy, acquiring cell death by the use of photosensitizer with a light, has been familiar for 100 years. First medical application of photodynamic therapy in literature was done by von Tappeiner and a dermatologist named Jesionek. They used topical eosin and white light for the treatment of skin cancer[10]. The requirement of oxygen in the reaction environment for the therapy was firstly introduced by Jodlbauer and von Tappeiner in 1907 and they entitled this phenomenon as "photodynamic action"[11].

In 1911, Hausmann reported the effect of hematoporphyrin and light on a paramecium and red blood cells of a mice[12]. Friedrich Meyer-Betz injected himself hematoporphyrin and exposed himself to light in order to observe the effects on humans as well as mice and he noticed long term pain at the areas where light has been exposed[13]. In 1978, with a 25 skin cancer patients were treated with PDT by Dougherty and this was the first clinical study which proved PDT can be used for the treatment of some malignant cancers more successfully than the conventional therapies[14].

Over the years PDT has been used successfully for the treatment of some other types of tumor such as, bladder cancer[15], brain tumors[16], head and neck tumors[17], rectal cancer[18], gynecological tumors[19].

1.1.2. Working Mechanism of Photodynamic Therapy

The activation of the photosensitizer with an appropriate wavelength of a light initiates the series of energy transfers. When the photosensitizer absorbs the light, it transfers from ground singlet state (^{1}PS) into its excited singlet state (^{1}PS*). ^{1}PS*

may either return back to ground state by fluorescence directly or it undergo electron spin conversion to its triplet state (^{3}PS*) which is needed to initiate photodynamic action. ^{3}PS* may undergo two different reaction types in the presence of O_2. In reaction Type I; the excited molecules transfer electron or proton to substrates and produce radicals or radical ions. Alternativeley in reaction Type II; excited photosensitizer transfers its energy to oxygen and cytotoxic singlet oxygen species ($^1O_2$) is produced[20].

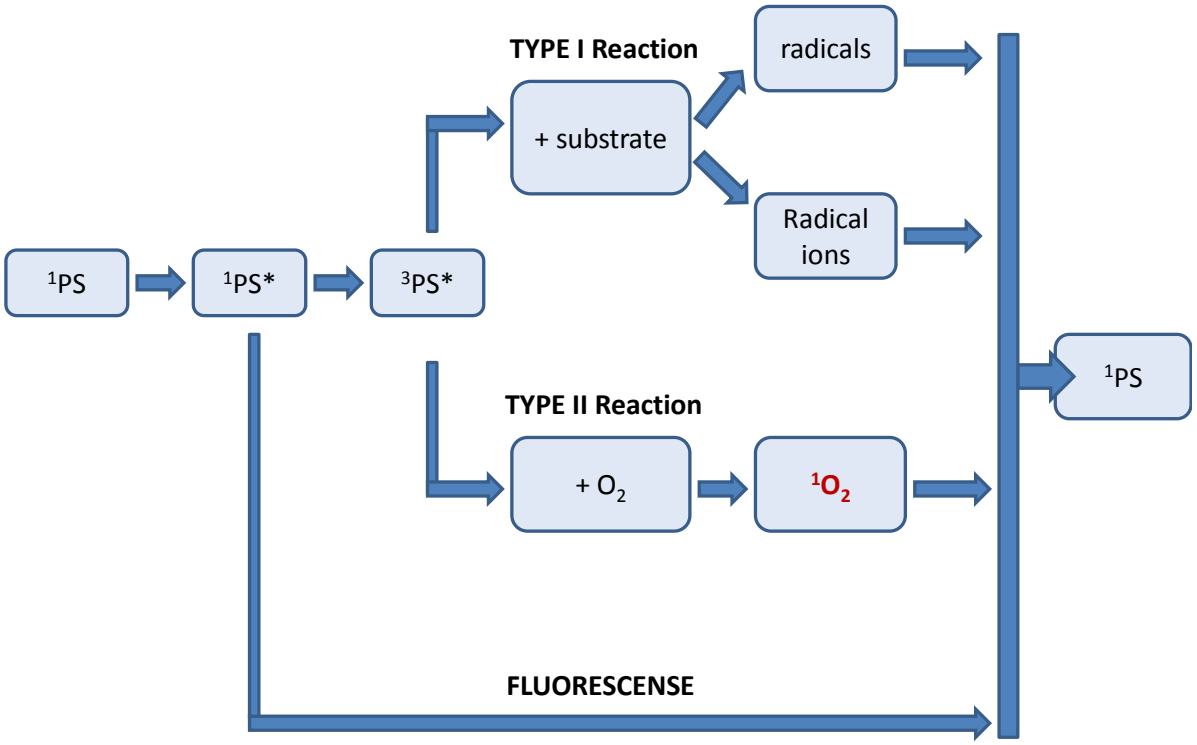

Figure 1. The principle of photodynamic therapy.

There are three different pathways that all come to the same result which is tumor death. $^1O_2$, which is generated by the series of photochemical reactions, may kill directly the tumor cells by inducing apoptosis and/or necrosis. It may also damage the vasculatory that surrounds the tumor and kill the tumor cells

indirectly[21]. In addition, after PDT treatment, the immune system is induced[22]. As a result, the immune response is initiated to kill the remaining tumor cells.

The vascular response, to kill the surrounding vasculatory of the tumor and making the tumor starving of oxygen and nutrients[23], is important however, researchers pay attention more to the effects of PDT in cellular level. The target sites of the cellular level include mitochondria, the plasma membrane, nuclei and lyzozomes[24]. The effectiveness of PDT is mainly resulted from the apoptotic response in cells. Apoptosis is programmed cell death due to the change of the biochemical environment of the cell. The mitochondrial damage is of top priority which leads to apoptosis [21, 25].

1.1.3. Photosensitizing Agents

The most ideal photosensitizing agents would have the properties such as, biostability, photochemically efficient (having a strong absorption peak at wavelengths >630nm), selective to target tissue (retain at the target tissue relatively more than normal surrounding tissues), minimum toxicity at the healthy parts of the body.

Photobleaching, destruction of the fluorescent molecules due to the generation of singlet oxygen species during the photodynamic action, is one of the main problems of photosensitizers[26]. As a result, photosensitizers must be photochemically stable.

Light penetration depth of the human tissue limits in the range of 620-850 nm because of the absorption properties of the medium[27] (Fig.2). This limited light penetration range is called as therapeutic window of the body. The photosenstizers must have a strong absorption in the region of the therapeutic window, thus they

can transfer their energy to oxygen in order to produce cytotoxic singlet oxygen species[28] .

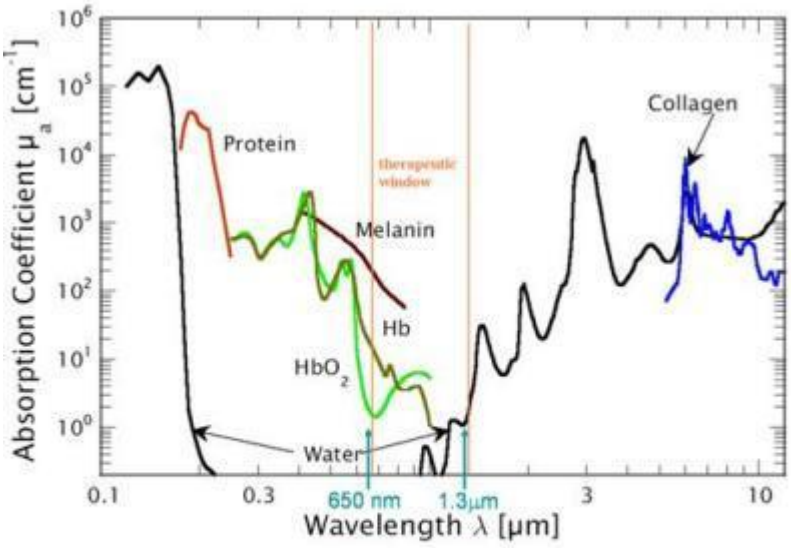

Figure 2. The optical absorption of various tissue components and therapautic window of body**.**

1.1.3.1 Clinical Studies of Photosensitizing Agents

Photofrin (porfimer sodium, Axcan Pharma, Montreal, Canada), a complex mixture of hematoporphyrin derivatives, is the first drug that was approved for PDT[7]. Since photofrin is very effective in terms of; killing the tumor, non-toxic when there is no illumination and water soluble, it is the most common photosensitizer for the treatment of some tumors other than dermatological. The cancers that are treated with photofrin are, early stage lung cancers, cervical cancer, bladder cancer, gastric cancer and oesophageal adenocarcinoma[28].

Although porfimer sodium is effective, it has several disadvantages which are improved in subsequent photosensitizers. The selectivity of the drug between tumors and healthy tissues is low[29]. After the administration of the porfimer sodium there should be waiting period of 48-72h before the illumination and since the drug causes skin photosensitivity during this period of time patient must be protected from light[30].

Research has been done to develop new photosensitizers which have improved properties over photofrin. Table 1 shows the approved photosensitizers and type of cancer they are applied.

Table 1. Type of cancer and approved drug[20]

TYPE OF CANCER	PHOTOSENSITIZER	COUNTRY
Actinic keratosis	ALA (Levulan, Metvix)	U.S., EU
Basal Cell Carcinoma	ALA (Metvix)	EU
Barrett's HGD	Porfimer sodium	U.S., Canada, EU, UK
Cervical Cancer	Porfimer sodium	Japan
Endobronchial Cancer	Porfimer sodium	Canada, UK,US,EU
Esophageal Cancer	Porfimer sodium	Canada, UK,US,EU
Gastric Cancer	Porfimer sodium	Japan
Head and Neck Cancer	Foscan	EU, Norway, Iceland
Papillary bladder Cancer	Porfimer sodium	Canada

Abbreviations: ALA, 5-aminolevulinic acid, HGD, high-grade dysplasia

The generality of photosensitizers in literature are hematoporphyrin derivatives. The structures of some photosensitizers in literature and their absorption wavelengths within the therapeutic window are given below (see Figure 2.)

Porphyrin derivatives

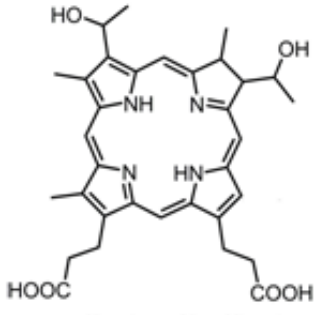

Hematoporphyrin
(Photofrin), 630nm

Phthalocyanines and naphtalocyanines

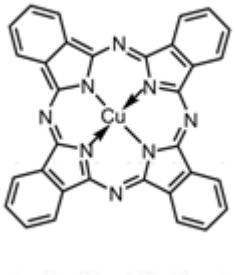

Phatalocyanine, 700nm

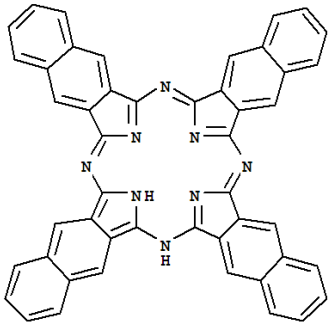

Naphthalocyanine, 780nm

Texapyrins

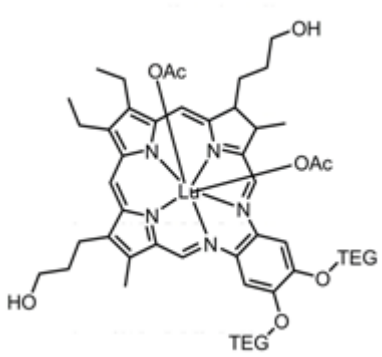

Texaphyrinato-Lu(III), 600-900nm

Chlorins and Bacteriochlorins

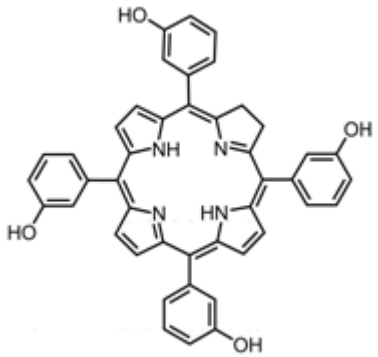

m-THPC,(*Foscan)*, 650nm

Aza dipyrromethene dyes

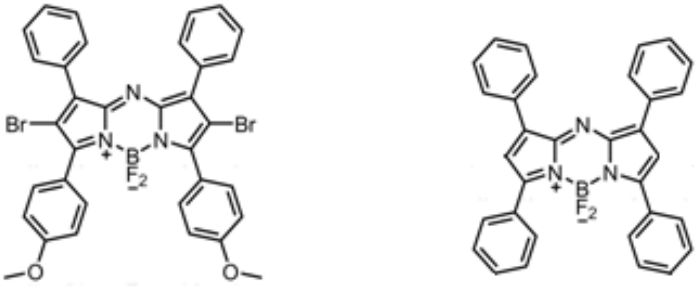

Aza dipyrromethene dyes, 650nm

Perylenediimide dyes

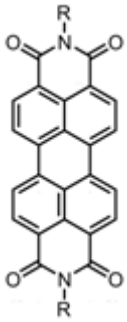

Boron dipyrromethene dyes

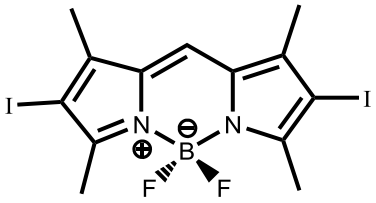

Figure 3. Structures of some photosensitizers in literature.

1.1.3.2 Boron dipyrromethene (BODIPY) dyes

4,4-Difluoro-4-bora-3a,4a-diaza-s-indacene (abbreviated to BODIPY) dyes are novel photosensitizers with the properties of high extinction coefficients, high quantum efficiencies of fluorescence and stability in physiological environment[31]. Possessing these advantageous properties, BODIPY dyes have become attractive in PDT research. One important point that draws interest on BODIPY dyes being able to modify them easily by attaching functional groups that can increase the selectivity of the dye to the target site. As they are used in imaging technologies by labeling proteins[32] and DNA[33] by the modifications on dye, they are used in PDT with increased targeting to tumor tissue[34]. In addition to targeting, one more advantage arises with the modification of the BODIPY dyes which is red shift in the absorption wavelength. Akkaya *et al.* synthesized four different styryl BODIPY dyes by stopping the reaction at appropriate time and observed the absorption and emission wavelength shifts successfully[35].

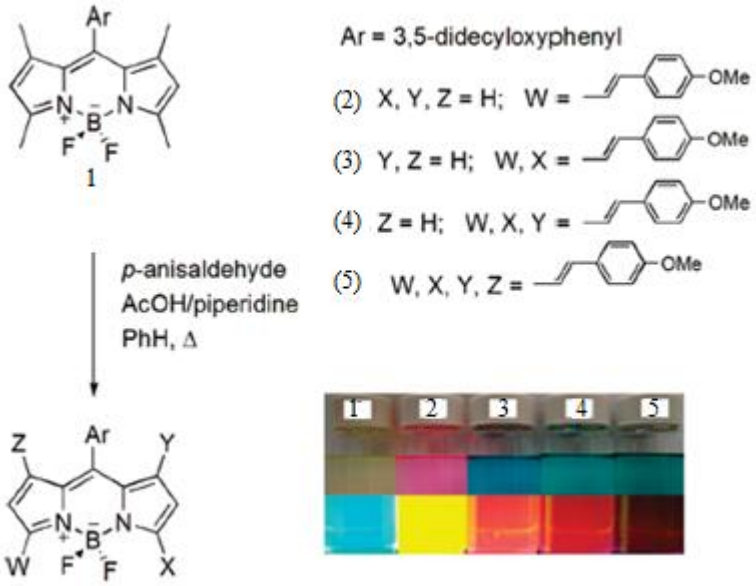

Figure 4. One-pot synthesis of different styryl BODIP dyes[35].

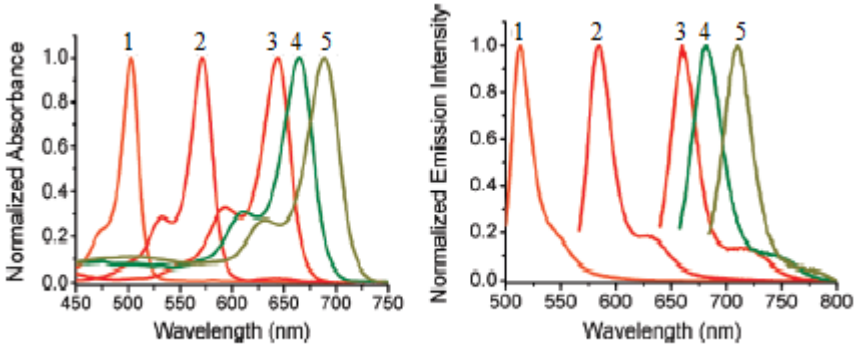

Figure 5. Absorption and emission spectra of styryl BODIPY dyes[35].

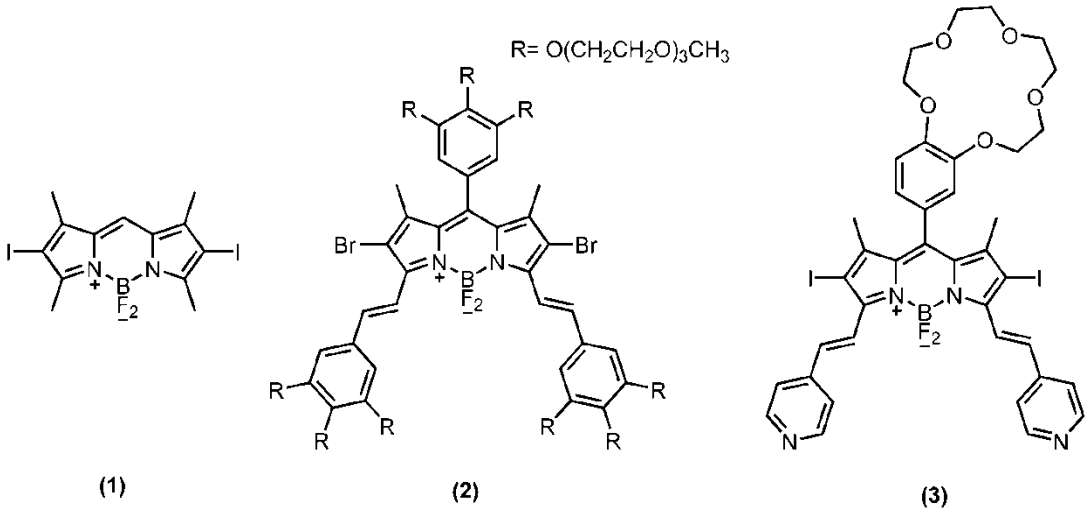

Figure 6. BODIPY- based photosensitizers in literature. Compound 1 is the first BODIPY-based photosensitizrs reported by Nagano et al., compound 2 and 3 were reported by Akkaya et al.35, 36, 34

The study of Akkaya *et al.*[34] is an important example of the modification of BODIPY for the tumor tissue environment. As it is previously discussed, tumor

tissues have abnormal physiological properties such as low pH, high concentration of Na^+ ion. The photosensitizer that was synthesized by Akkaya *et al.* (compound **3** in fig. 6) has two different functional groups which are sensitive to acidicity and sodium ion concentration. In the acidic medium, pyridine groups are protonated and red shift occurs from 630 nm to 660 nm. Thus, only the protonated molecules would absorb light at 660 nm. In the absence of sodium ion, photo induced electron transfer (PET) occurs however when the sodium ion concentration increases, sodium ion binds to crown ether group of the molecule and PET is blocked. By this way, only in the tumor tissues where the two parameters are above a threshold value, the $^1O_2$ species would be generated. (Fig. 7)

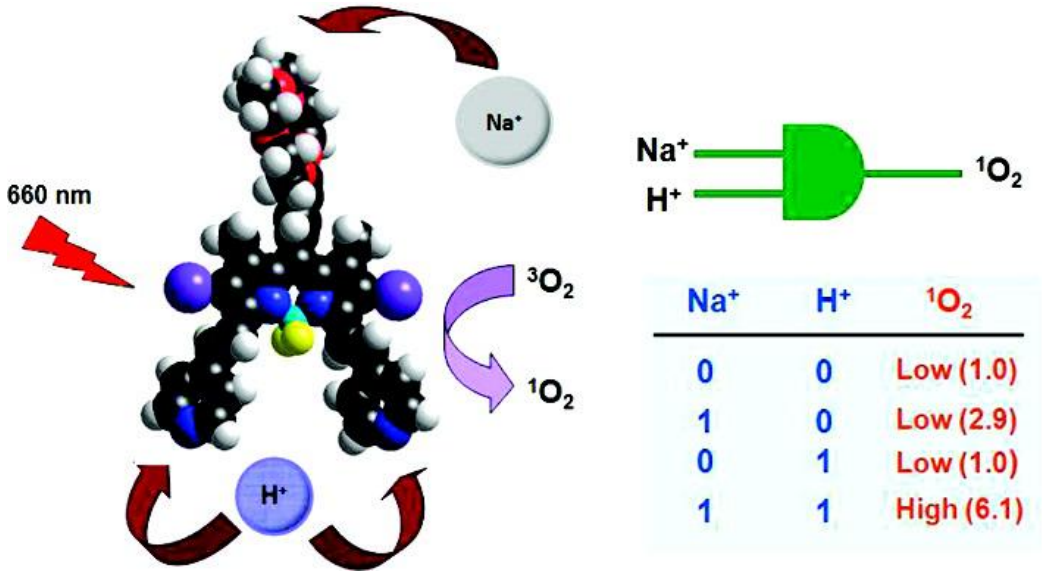

Na^+	H^+	$^1O_2$
0	0	Low (1.0)
1	0	Low (2.9)
0	1	Low (1.0)
1	1	High (6.1)

Figure 7. Smart photosensitizer that is selective to tumor tissue environment[34].

1.1.4. Light Sources

For the activation of photosensitizers, conventional arc lamps can be used. They are cheap and easy to use, however they are broad spectrum light sources so filters should be used to cut off UV and IR emission to avoid heating. In addition, while coupling them to light delivery fibers, there occurs optical power loss. Thus, it is not efficient to use arc lamps clinically.

The development of lasers is an important breakthrough in PDT because early lasers were expensive, large and cannot removable and expertise is needed to use them. The development in semiconductor lasers results in cheaper, mobile systems that can be used corporately with optical fiber technology. For PDT to be successful, the light should be delivered from source to target homogenously, thus the optical fibers provide the needs for illumination at different localization.

Light emitting diodes (LEDs) can also be used clinically. They are small, cheaper than the other light sources and provide a power output up to 150mW/cm^2 at wavelengths between 350-1100 nm[37].

1.2 Requirements for Drug Delivery Systems

Over the last decades, many organic dyes, porphyrin derivatives and other biomolecules have been synthesized as photosensitizing agents. However, developments in photosensitizing agents yet could not solve all the problems for the clinical applications.

First of all, most of the photosensitizing agents are hydrophobic so they are water insoluble molecules. Thus, in aqueous media they aggregate easily which in turn results in two important issues, decrease in quantum efficiency and severity at injection through the body.

Secondly, to prevent the damage of healthy tissues selective accumulation of photosensitizing agent is required. Although, recently photosensitizers are synthesized in order to increase selective targeting, they are still not selective enough to be applied clinically.

As a result, the construction of stable and effective photosensitive agent carriers become vital and play an important role for the development of PDT. The common examples of delivery agents are liposomes, oil dispersions, low-density lipoproteins and nanoparticles[38,39].

1.2.1 Nanoparticles as photosensitizer carriers for PDT

Recently, nanotechnology focuses on development of nanoparticles as photosensitizer carriers. Nanomaterials are promising in PDT issue because (1) they could be made water soluble, i.e. hydrophilic, (2) they have large surface areas which can be modified with functional groups, thus gain selectivity for the tumor tissue, (3) they have sub-cellular size so they can easily penetrate deeper into the tissue and are efficiently taken up by the cell.

PS agent could be encapsulated within their matrix, adsorbed on the material or conjugated on the surface. Since the surface of these nanoparticles is ready for modification, tumor seeking sites can be attached to the surface of them which provides specific targeting. In addition, attachment of a different fluorescent molecule provides biological imaging of the system.

There are various types of nanomaterials that can be used as PS carrier systems, organic compounds, inorganic oxides, metal compounds.

1.3. Mesoporous silica nanoparticles (MSNs) as PS carrier

Research on ceramic based nanomaterials as a drug carrier system for PDT has been done recently. Synthesis of organically modified silica nanoparticles (ORMOSIL) was first reported by Ohulchanskyy *et al.* According to Ohulchanskyy and his colleagues, this novel nanoparticles consist of silica nanoparticles and covalently incorporated photosensitizer HPPH (2-devinyl-2-(1-hexyloxyethyl)pyropheophorbide) for PDT[40] . Zhang *et al.* reported photosensitizer carrier system for PDT in which PS absorbs infrared light based on photon upconverting nanoparticles (PUNPs) coated with silica matrix[41].

During the last decade, research has done to develop mesoporous materials. Possessing the good properties such as being chemically inert, thermally stable in biological environment, harmless for human body and inexpensive, silica is the well developed mesoporous material[42].

Mesoporous silica particles were first described and patented by French scientists in 1967[43]; however it was not noticed until 1990's. In 1989 Kato *et al.* reported microporous silica particles which were synthesized by using kanemite as starting material[44]. In 1992, Kresge *et al.* firstly introduced MCM-41, mesoporous crystalline materials, at Mobil Research and Development Corporation Laboratories[45]. Following this study, there were a few achievements which mainly introduced new types of mesoporous silica nanoparticles with different pore size distributions[46,47].

There are many procedures to synthesize different size and pore distribution MCM series. The most commonly used synthesis pathway is the organic template driven one[48]. A template is an agent which directs a structure. It is often a molecule or ion around which a framework is built. They are used for the synthesis of large number of zeolites and the most common ones are quaternary ammonium ions with a short alky chains. For the synthesis of MCM-41, quaternary ammonium ions with a long alkyl chain, generally hexadecyl group, are used as a template. In aqueous media, the long hydrophobic alkyl chain of the template would aggregate in order to minimize the interaction of the hydrophobic chain with highly polar water molecules. This aggregation results in the formation of micelles. These micelles have hydrophilic surface due to the ionic character of ammonium and hydrophobic core consists of large alkyl chains. In order to minimize the surface energy, micelles tend to form a spherical shape. However, as the number of templates increase in aqueous media, micelles evolved into different geometry. These micelles have new shape of long tubes, often denoted as rod-like micelles. When the concentration of templates even becomes higher, they aggregate and form hexagonal liquid crystalline structure which resembles the MCM-41 structure[49].

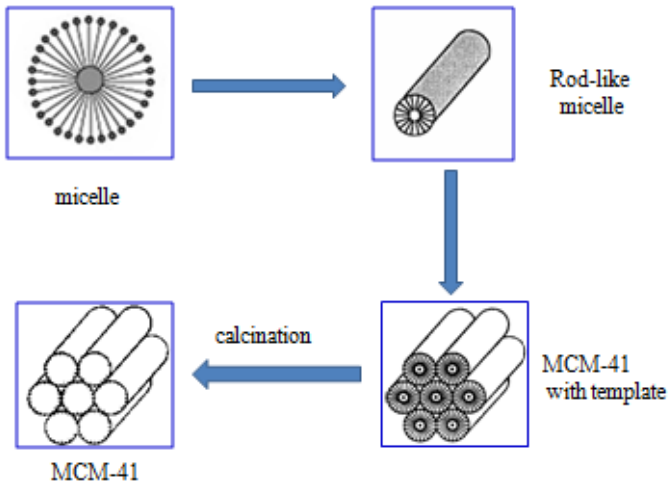

Figure 8. Synthesis pathway of MCM-41[46].

CHAPTER 2

EXPERIMENTAL PROCEDURES

2.1 General

All chemicals and solvents purchased from Sigma-Aldrich and they were used without further purification. ^{1}H NMR and ^{13}C NMR data were obtained using Bruker DPX-400 in $CDCl_3$ with TMS as internal reference. Splittings in spectra are shown as s (singlet), d (doublet), t (triplet), q (quartet), m (multiplet). Column chromatography for all products was performed by using Merck Silica Gel 60 (particle size: 0.040- 0.063 mm, 230-400 mesh ASTM).

Mass spectrometry was performed using MS-QTOF at Bilkent University, UNAM, Mass Spectrometry Facility.

Absorption spectrometry was performed using Varian UV-Vis-NIR Spectrophotometer. Fluorescence emission spectra were obtained by using Varian Eclipse spectrofluorometer.

Particle size and zeta potential data were acquired by using Malvern Zetasizer Nanoseries at Bilkent University, UNAM, Ankara.

XRD data were obtained by using PANalytical X'Pert Pro MPD Multi-purpose X-ray diffractometer at Bilkent University, UNAM, Ankara.

SEM images were acquired in UNAM, Ankara, using Quanta 200 FEG, Environmental Scanning Electron Microscopy. TEM images were obtained in UNAM, Ankara, using FEI Technai G2 F30 high resolution transmission electron microscope and carbon grid.

Analysis of Nitrogen Adsorption was done at METU, Central Laboratory, Surface Characterization Unit, Ankara, by using Quantachrome Corporation, Autosorb-6.

2.2 Synthesis of Photosensitizer

2.2.1 Synthesis of 4-(3-bromopropoxy)benzaldehyde (3)

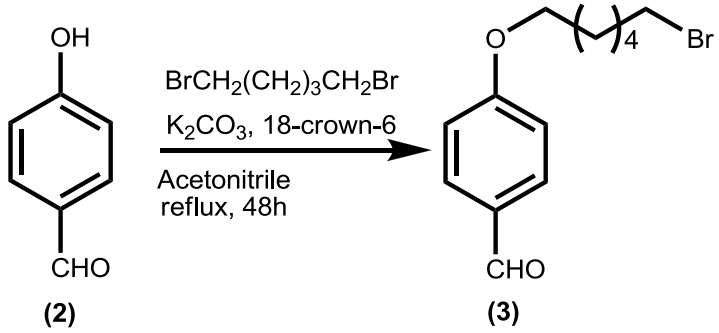

Figure 9. Synthesis of compound **3**

Hydroxybenzaldehyde (2 g, 16.4 mmol) and 1,6 dibromohexane (5.2 ml, 32.8 mmol) were dissolved in acetonitrile (150ml). K_2CO_3 (6.88 g, 49.2 mmol) and a few crystals of 18-crown-6 were added. The reaction mixture was refluxed for 48 h. Then acetonitrile was evaporated in vacuum and extracted with water and chloroform. Organic phase was dried with Na_2SO_4 and evaporated by using rotary evaporator. The product was purified by silica gel column chromatography using $CHCl_3$/Hexane (5:1, v/v). Fraction containing product **3** was collected then the solvent was removed by using rotary evaporator. (2.4 g, 8.4 mmol, 51%).

^{1}H NMR ($CDCl_3$, 400MHz, δ ppm) 1.45 (m, 4H), 1.75 (t, *J*= 6.7Hz, 2H), 1.82 (t, *J*= 6.9Hz, 2H), 3.32 (t, *J*= 6.7Hz, 2H), 3.95 (t, *J*= 6.4Hz, 2H), 6.89 (d, *J*= 8.8Hz, 2H), 7.73(d, *J*= 8.7Hz,2H), 9.80 (s,1H)

2.2.2 Synthesis of 4-(3-azidopropoxy)benzaldeyhde (4)

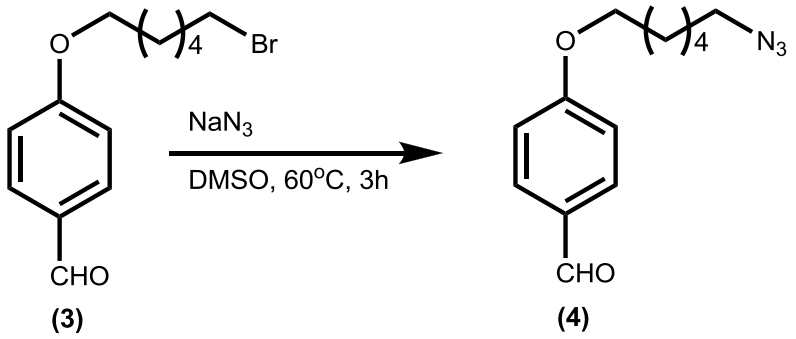

Figure 10. Synthesis of compound **4**

4-(3-Bromopropoxy)benzaldehyde (**3**, 1.5 g, 5.3 mmol) was dissolved in DMSO (25ml), NaN_3 (1.37 g, 21.2 mmol) was added. Reaction mixture was heated to 60°C for 3 hours. Extraction was done several times with water and chloroform to get rid of DMSO. After the extraction, organic phase was dried with Na_2SO_4 and evaporated by using rotary evaporator. The residual compound was liquid at room temperature and pure.

^{1}H NMR ($CDCl_3$, 400MHz, δ ppm) 1.30-1.45 (m, 4H), 1.55 (t, *J*= 6.4Hz, 2H), 1.72 (t, *J*= 6.5Hz, 2H), 3.20 (t, *J*= 6.9Hz, 2H), 3.95 (t, *J*= 6.4Hz, 2H), 6.90 (d, *J*= 8.7Hz, 2H), 7.72 (d, *J*= 8.9Hz, 2H), 9.75 (s, 1H)

2.2.3 Synthesis of 8-(4-(6-azidohexyloxy)phenyl)-1,3,5,7-tetramethyl-BODIPY (5)

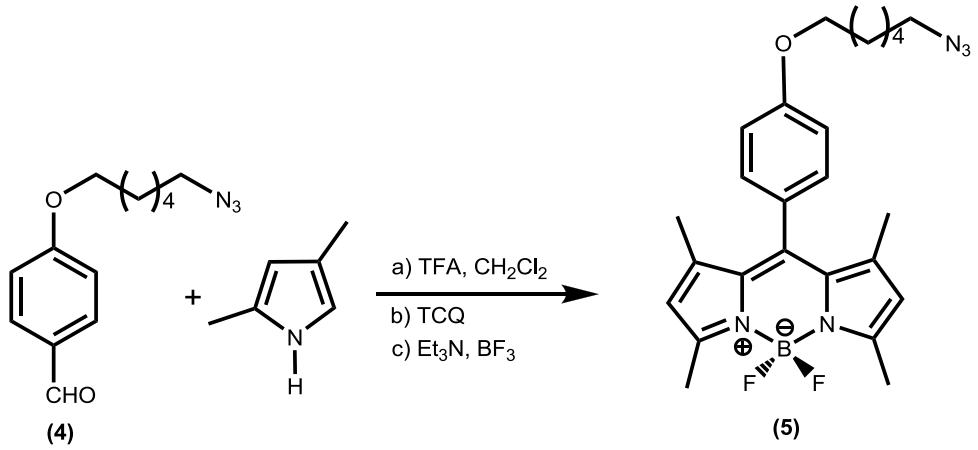

Figure 11. Synthesis of compound **5**

CH_2Cl_2 (200 ml) was purged with Ar for 20 minutes. 4-(3-azidopropoxy)benzaldeyhde **4** (0.7 g, 2.85 mmol) and 2,4-dimethyl pyrrole (0.65 g, 5.7 mmol) were added. 3 Drops of trifluoroacetic acid was added and the color of reaction mixture was turned into red. The reaction mixture was stirred at room temperature for 12h. Then tetrachloro-1,4-benzoquinone (0.7 g, 2.65 mmol) was added ant the reaction mixture stirred at room temperature for 45 min. Then triethyl amine (3 ml) and borontrifluoride diethyl etherate were added respectively. After stirring at room temperature for 45 minutes, extraction was done with water. Organic phase was dried with Na_2SO_4 and evaporated by using rotary evaporator. The purification was done by silica gel column by using chloroform. Fraction that contains compound **5** was collected then the solvent was evaporated by using rotary evaporator. (0.69 mmol, 25%).

^{1}H NMR ($CDCl_3$, 400MHz, δ ppm) 1.42 (s, 6H), 0.45-1.62 (m, 4H), 1.65 (t, *J*= 7.2, 2H), 1.85 (t, *J*= 7.3, 2H), 2.55 (s, 6H), 3.30 (t, *J*= 6.8, 2H), 4.03 (t, *J*= 6.4, 2H), 6.00 (s, 2H), 7.00 (d, *J*= 4.6), 7.18 (d, *J*= 4.6)

^{13}C NMR ($CDCl_3$, 100MHz, δ ppm) 14.6, 25.7, 26.6, 28.8, 29.1, 51.4, 67.9, 115.0, 121.2, 126.8, 129.2, 130.4, 131.8, 141.9, 143.2, 155.2, 159.6

HRMS-ESI: calculated for M+H 466.3464, found 466.2573, Δm= 19 ppm

2.2.4 Synthesis of 8-(4-(6-azidohexyloxy)phenyl)-2,6-dibromo1,3,5,7-tetramethyl-BODIPY (6)

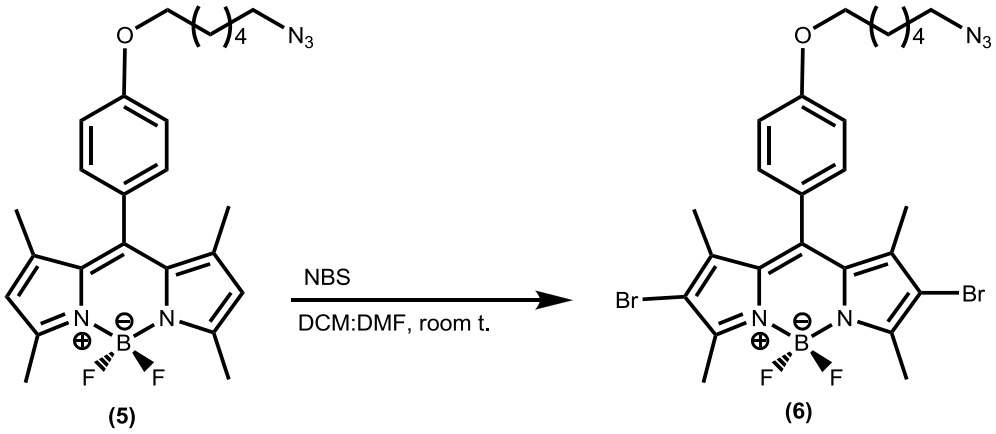

Figure 12. Synthesis of compound **6**

10-(4-(6-azidohexyloxy)phenyl)-2-8-dibromo-5,5-difluoro-1,3,7,9-tetramethyl-5H-dipyrrolo[1,2-c:1',2'-f] [1,3,2]diazaborinin-4-ium-5-uide **6** (322 mg, 0.69 mmol) was dissolved in a mixture of DMF/DCM (25ml:25ml). Then N-bromo succinimide (370 mg, 2.07 mmol) was dissolved in DCM (25ml). NBS in DCM solution was

added to the reaction solution dropwise in 15 min. The reaction mixture was stirred at room temperature for 2 hours. Followed by thin layer chromatography the reaction was stopped and the extraction was done with water and DCM. The organic phase was dried with Na_2SO_4 and evaporated by using rotary evaporator. The purification was done by silica gel column by using chloroform/ hexane mixture (3:1 v/v). Fraction that contains compound **6** was collected then the solvent was evaporated by using rotary evaporator. (150 mg, 0.239 mmol, 35%)

^{1}H NMR ($CDCl_3$, 400MHz, δ ppm) 1.42 (s, 6H), 1.45-1.62 (m, 4H), 1.65 (t, *J*= 7.2, 2H), 1.85 (t, *J*= 7.3, 2H), 2.60 (s, 6H), 3.30 (t, *J*= 6.8, 2H), 4.03 (t, *J*= 6.4, 2H), 7.00 (d, *J*= 4.6, 2H), 7.18 (d, *J*= 4.6, 2H)

^{13}C NMR ($CDCl_3$, 100MHz, δ ppm) 13.7, 13.9, 25.7, 26.3, 27.0, 28.8, 29.1, 51.4, 68.0, 115.3, 126.3, 129.1, 130.8, 140.6, 142.4, 153.7, 160.1

HRMS- ESI: calculated for M+H 622.07, found 622.0727 Δm= 4.3 ppm

2.2.5 Synthesis of compound 7

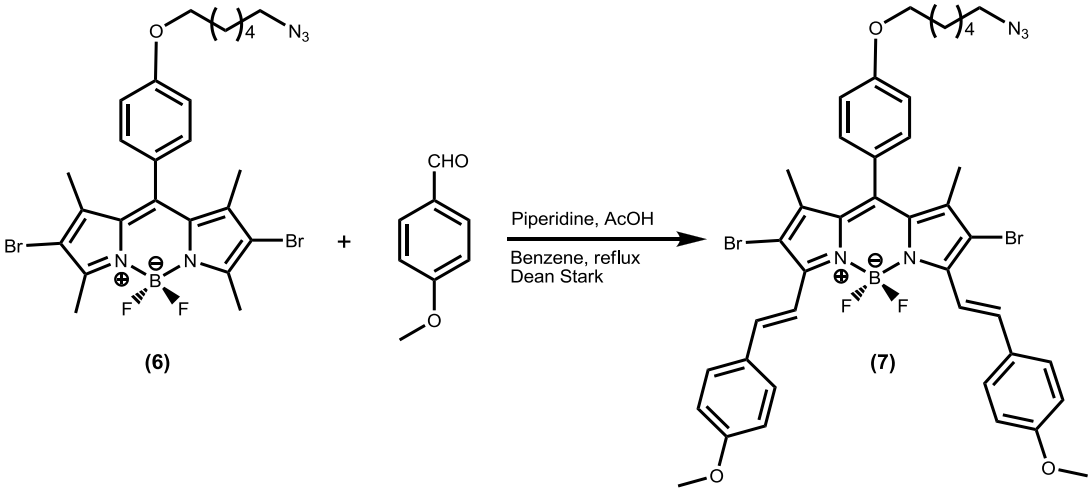

Figure 13. Synthesis of compound **7**

Compound **6** (100 mg, 0.160 mmol) and 4-methoxybenzaldehyde (55mg, 0.40 mmol) dissolved in benzene (50 ml). Piperidine (0.4 ml) and glacial acetic acid (0.4 ml) were added respectively. The solution was refluxed by using Dean-Stark apparatus. When the amount of solvent remained in the solution was minimized, the reaction was followed by TLC until observing the green colored product had the major band. Then the reaction was stopped and the extraction was done with chloroform and water. The organic phase was dried with Na_2SO_4 and evaporated by using rotary evaporator. The purification was done by silica gel column by using chloroform as mobile phase. Fraction containing compound **7** was collected then the solvent was evaporated under reduced pressure. (90 mg, 0.105 mmol, % 66)

^{1}H NMR ($CDCl_3$, 400MHz, δ ppm) 1.50 (m, 4H), 1.50 (s, 6H), 1.65 (t, *J*= 7.1 Hz, 2H), 1.90 (t, *J*= 7.2, 2H), 3.30 (t, *J*= 6.8, 2H), 3.88 (s, 6H), 4.08 (t, *J*= 6.3, 2H),

6.95 (d, *J*= 8.8, 4H), 7.04 (d, *J*= 8.6, 2H), 7.19 (d, *J*= 8.6, 2H), 7.65 (m, 2H+4H), 8.12 (d, *J*= 16.6, 2H)

^{13}C NMR ($CDCl_3$, 100MHz, δ ppm) 13.9, 15.4, 22.7, 25.8, 26.7, 29.2, 29.7, 31.6, 51.34, 55.4, 65.8, 68.0, 109.9, 114.4, 115.3, 116.2, 126.8, 129.3, 129.8, 132.48, 138.9, 141.0, 148.4, 160.0, 160.9

2.2.6 Synthesis of 3-isothiocyanatoprop-1-yne (8)

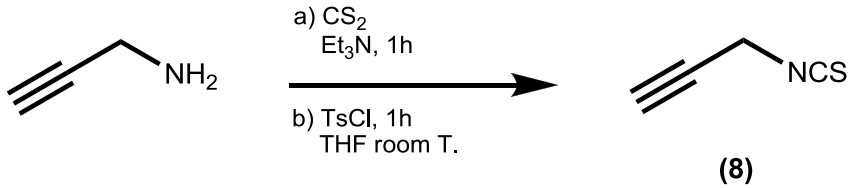

Figure 14. Synthesis of compound **8**

Propargyl amine (401.5 ml, 7.3 mmol) and triethyl amine (2216 mg, 21.9 mmol) was added to THF solution (10 ml) and the solution was cooled with an ice bath under Ar for 30 minutes. Then CS_2 (556 mg, 7.3 mmol) was added to the reaction mixture dropwise over 30 minutes with vigorous stirring. After the addition was completed, the mixture was stirred at room temperature for 1 h. Then, the reaction mixture was cooled with an ice bath and TsCl (1540 mg, 8.103 mmol) was added and then stirred for half an hour at room temperature.

At last, HCl (1N, 10ml) and diethylether (10ml) were added to the solution and extracted several times with small amount of diethyl ether. The organic phase was

dried with Na_2SO_4 and evaporated under reduced pressure. The purification was done by silica gel column by using hexane/chloroform mixture (10:1.5 v/v) as mobile phase. Fraction containing compound **8** was collected then the solvent was evaporated by rotary evaporator. The residual was yellow liquid with odor. (400 mg, 4.1 mmol, %56)

^{13}C NMR ($CDCl_3$, 100MHz, δ ppm) 14.1, 31.6, 35.0, 73.8

HRMS-ESI: calculated 97.00, found 96.9592 Δm= 42 ppm

2.2.7 Synthesis of Compound 9 (Click Reaction)

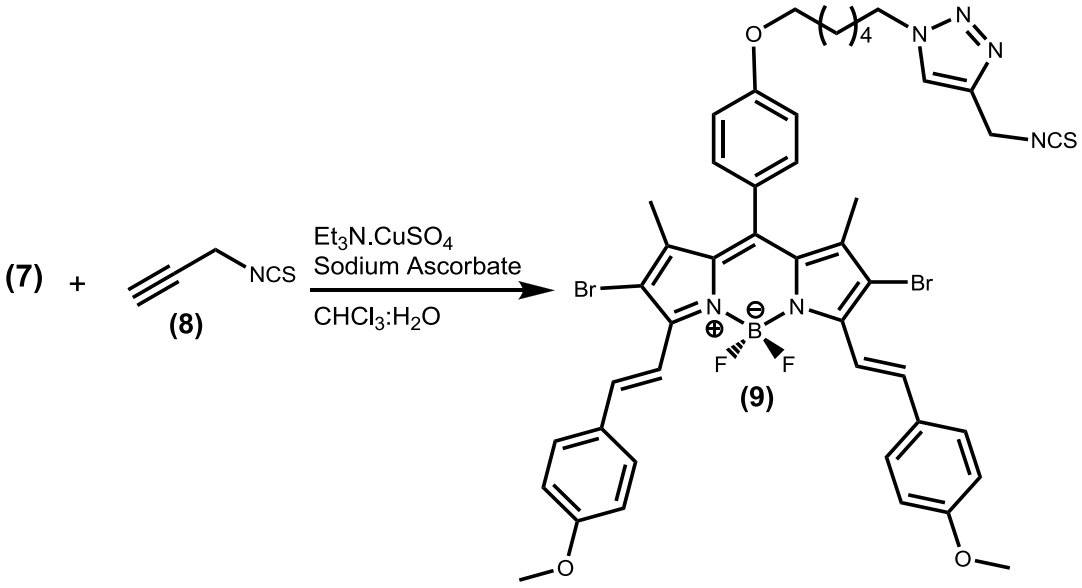

Figure 15. Synthesis of compound **9**

Synthesis was done following the procedure in literature[50]. Compound **7** (80 mg, 0.093 mmol) and compound **8** (27 mg, 0.279 mmol) was dissolved in $CHCl_3$ (6 ml). A few drops of triethyl amine were added to the reaction and the mixture was stirred for 5 minutes at room temperature. In a vial, $CuSO_4$ (5 mg) dissolved in water (0.7 ml). In another vial, sodium ascorbate (8 mg) was dissolved in water (0.7 ml). $CuSO_4$ and sodium ascorbate solutions were added to the reaction mixture in turn. The reaction mixture was stirred at room temperature for 48 h. Then the extraction was done with $CHCl_3$ and water. Organic layer was dried with Na_2SO_4 and evaporated under reduced pressure. The purification was done by silica gel column by using $CHCl_3$ as mobile phase. Fraction was collected and the solvent was removed by using rotary evaporator. (20 mg, 0.021 mmol, 23%)

^{1}H NMR ($CDCl_3$, 400MHz, δ ppm) 1.30 (m, 4H), 1.50 (s, 6H), 1.85 (t, *J*= 7.9 Hz, 2H), 2.05 (t, *J*= 7.5, 2H), 3.88 (s, 6H), 4.05 (t, *J*= 6.4, 2H), 4.43 (t, *J*= 7.2, 2H), 4.88 (s, 2H), 6.82 (d, *J*= 8.8, 4H), 7.04 (d, *J*= 8.6, 2H), 7.19 (d, *J*= 8.6, 2H), 7.65 (m, 2H+4H+1H), 8.14 (d, *J*= 16.6, 2H)

^{13}C NMR ($CDCl_3$, 100MHz, δ ppm) 14.0, 25.6, 26.6, 29.1, 29.8, 30.3, 41.1, 50.7, 55.5, 67.9, 114.3, 115.3, 116.2, 121.6, 126.9, 128.8, 129.3, 129.7, 129.88, 130.93, 132.5, 138.8, 141.0, 148.4, 160.0, 160.8

MALDI: calculated 956.54 and found 956.16

2.2.8 Synthesis of MSNs

The synthesis was done according to the procedure in literature[53] . Cetylammonium bromide (CTAB) (0.1g) was dissolved in NH_4OH (50 g, 0.51 M) at 50^{o}C and tetraethyl orthosilicate (TEOS) (0.8 ml, 0.2 M in ethanol) was added under continous stirring. After stirring 5 hours, 3-aminopropyltrimethoxysilane (APTMS) (0.8 ml of 12% (v/v) in ethanol) and TEOS (0.8 ml of 1M) were added to the solution and stirred for 1 hour. The solution was stirred for 24 hours at 50^{o}C.

The solution was centrufuged and the precipitates were collected by washing with deionized water and ethanol several times. In order to remove surfactant templates particles were added to acidic ethanol (3 ml concentrate HCl in 100 ml of ethanol) and stirred 24 hours at 65 ^{o}C.

2.2.9 Synthesis of PS-MSNs

Compound **9** (10 mg) was added into distilled THF (6 ml). MSNs (60 mg) was added to the reaction mixture and the mixture was stirred for 2 days at room temperature. After 2 days, the mixture was centrufuged and washed with chloroform to get rid off the unreacted compound **9**. This process was continued until there observed no color in the solution of centrufuged mixture.

The solid particles were taken and were left to dry at room temperature.

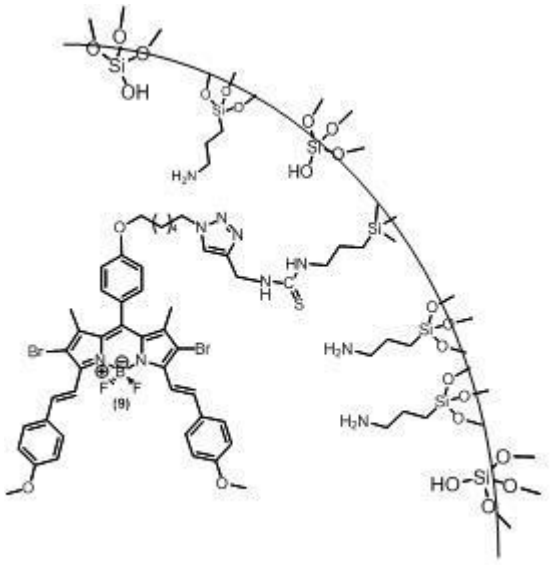

Figure 16. Schematic drawing of PS-MSNs

CHAPTER 3

RESULTS AND DISCUSSION

3.1 MSNs as a Carrier System for Photosensitizer

Mesoporous silica nanoparticles are convenient carrier system for drugs when their unique properties such as; large surface areas, uniform pore sizes, hydrophilicity, acquiring targeting by surface modification and low cytotoxicity are considered. Photodynamic therapy, treatment of cancer cells by using photosensitizers along with light, growing interest of research recently. This way of therapy has numerous advantages over other types of cancer treatment. Since PDT maintains the treatment of tumors locally, it minimizes the damages to the surrounding healthy tissue. Photosensitizers tend to localize in cancer tissues more than the healthy tissues and the exposure of light to only cancer tissue provides further selectivity.

3.1.1 Design of Photosensitizer

In this study, we have designed a novel photodynamic therapy reagent based on BODIPY derivative where MSNs are used as carrier system. The reason for selecting BODIPY as photosensitizer is its stability under light, high extinction coefficient and ease of modification of its core. For instance, modification of BODIPY at 1,3,5,7 positions with styryl groups was reported by Akkaya et al. recently[35]. Here, we modified 3, 5 positions by Knoevenagel condensation reactions

and obtained distyryl-BODIPY. The aim of this modification was to move absorption and emission bands of the compund further into the red end of the visible spectrum.

Bromination of the 2, 6 positions were done in order to increase spin-orbit coupling by introducing heavy atom. With this modification, transition from singlet excited state of photosensitizer to triplet state is enhanced[51]. In order to attach photosensitizer to mesoporous silica nanoparticles, isothiocyanate functional group was attached to photosensitizer by click reaction. Characterization of all compounds were done by using ^{1}H and ^{13}C NMR spectra and Mass spectrometry analysis and are given in the appendices A and B.

The absorbance maxima of the photosensitizer is at 653 nm which is convenient for photodynamic therapy since it is in the range of therapeutic window of body. (Figure 17.) The fluorescence emission maxima is at 678 nm (Figure 18.).

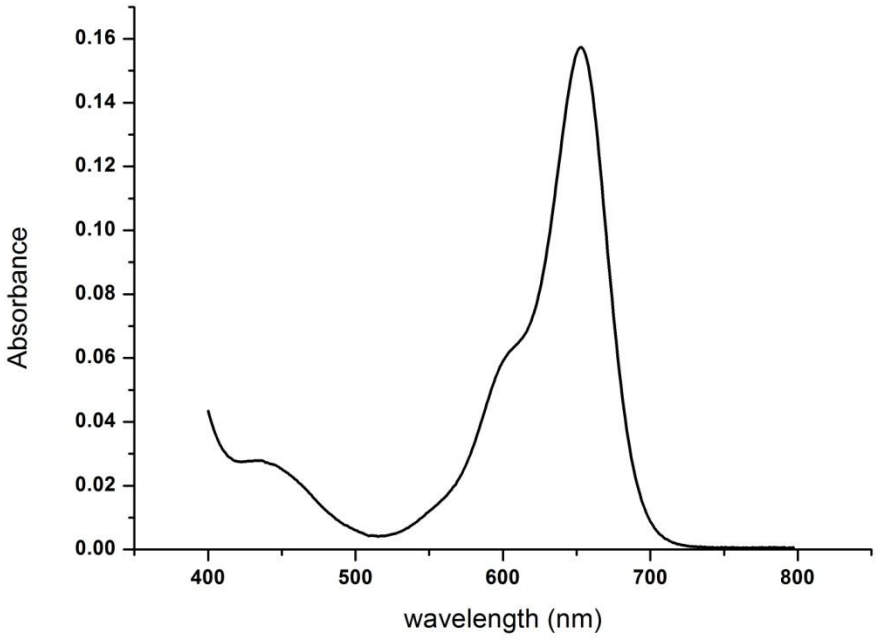

Figure 17. Absorbance of compound **9** in CHCl3

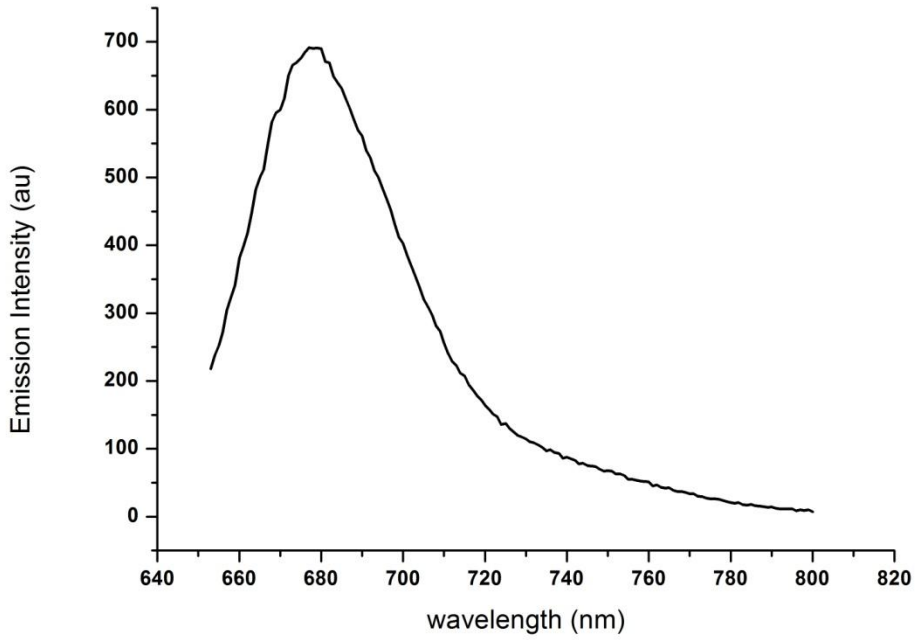

Figure 18. Fluorescense emission of compound **9** in $CHCl_3$. Excitation is at 650 nm.

3.1.2 Design of MSNs

MSNs were sytnhesized with low-concentration of TEOS, CTAB as surfactant and base-catalyst NH_4OH. In order to modify the surface of MSNs with photosensitizer, MSNs-APTS was synthesized. For this aim, sol gel process was applied by co-condensation of TEOS with APTS (3-aminopropyl-trimethoxy silane). The as synthesized particles were characterized by several characterization methods.

The size of the particles were measured as approximately 100 nm by using scanning electron microscopy (SEM). (Figure 19)

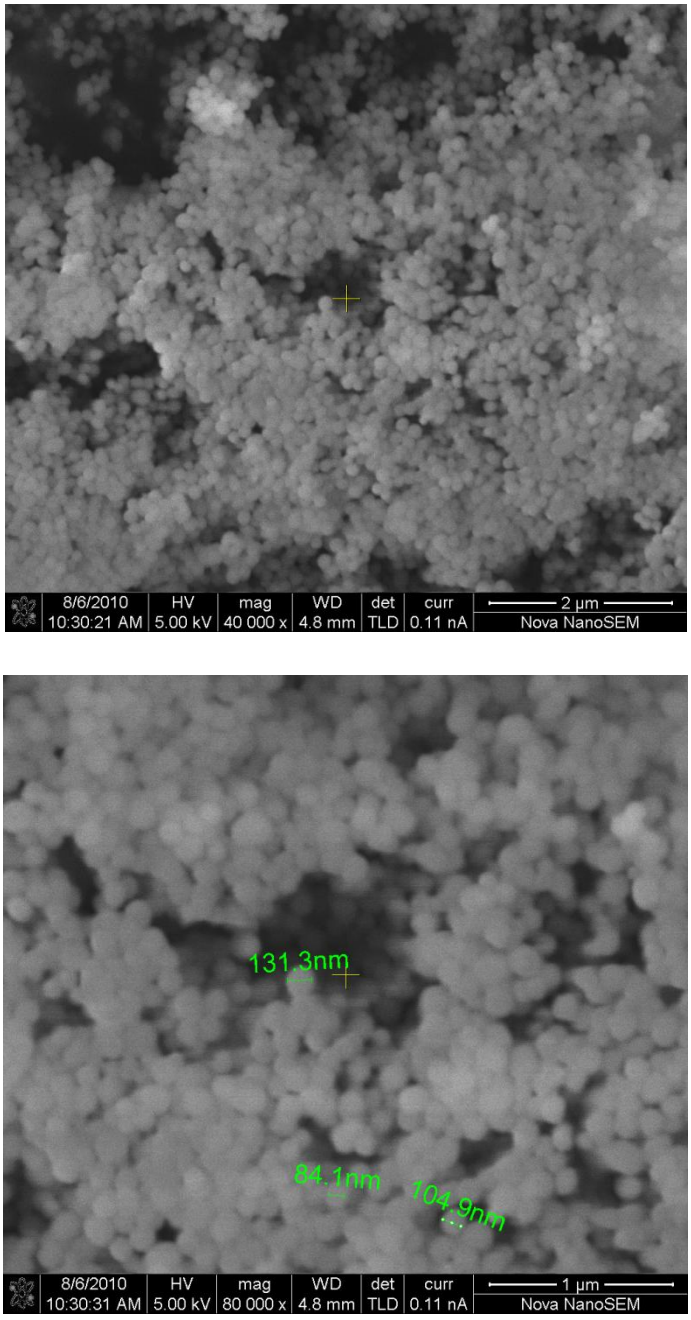

Figure 19. SEM images of MSNs

Mesoporous surface of the particles can be seen in the images obtained by using transmission electron microscopy (TEM) (Figure 20.)

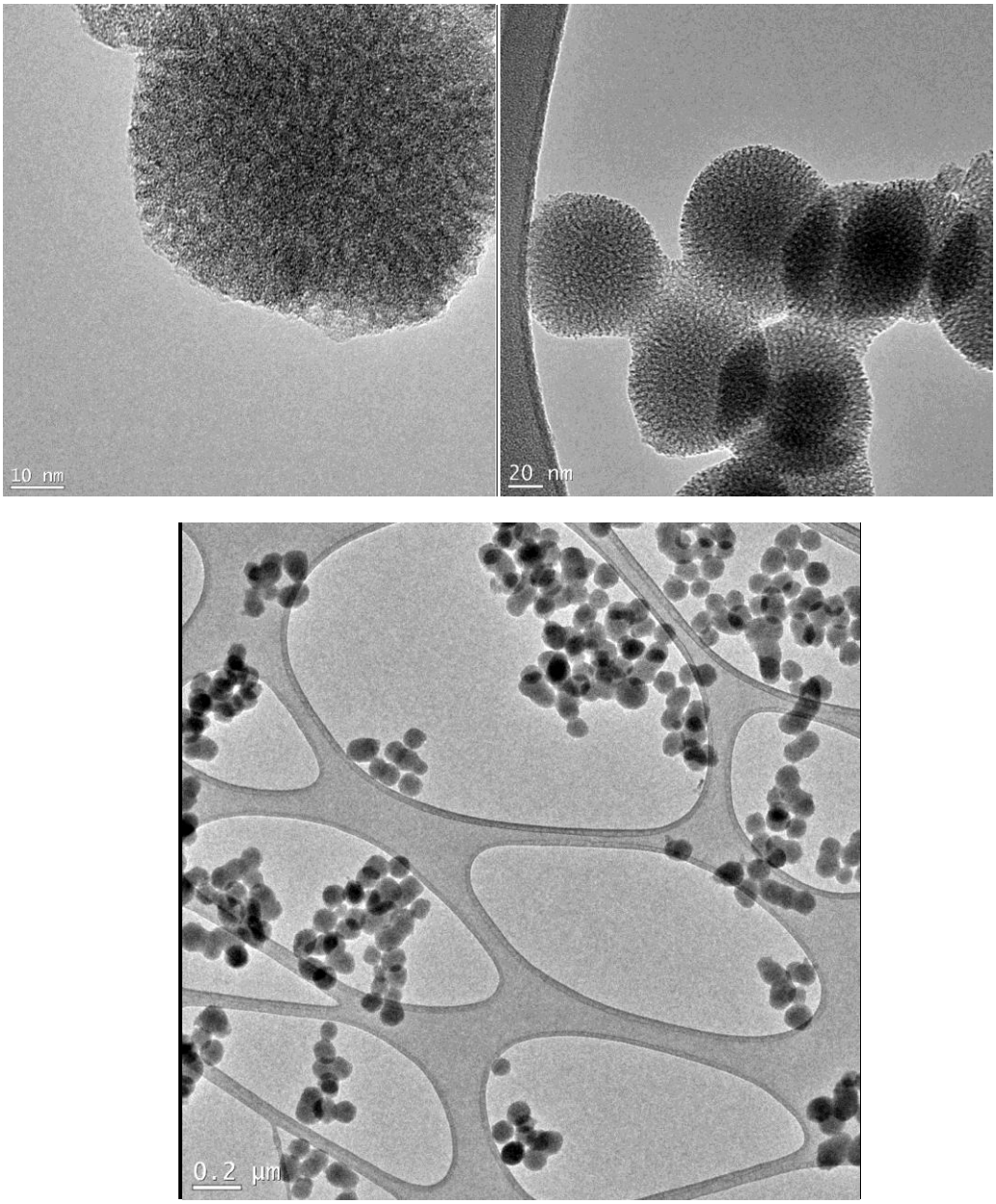

Figure 20. TEM images of MSNs

X-ray diffraction characterization shows that MSNs have well-ordered lattice. The geometry of the lattice shows that MSNs have hexagonal unit cell. This type of MSNs is MCM-41. Because the parameters of the unit cell is just in order of few nanometers, the x-ray diffracted on small angles. (Figure. 21)

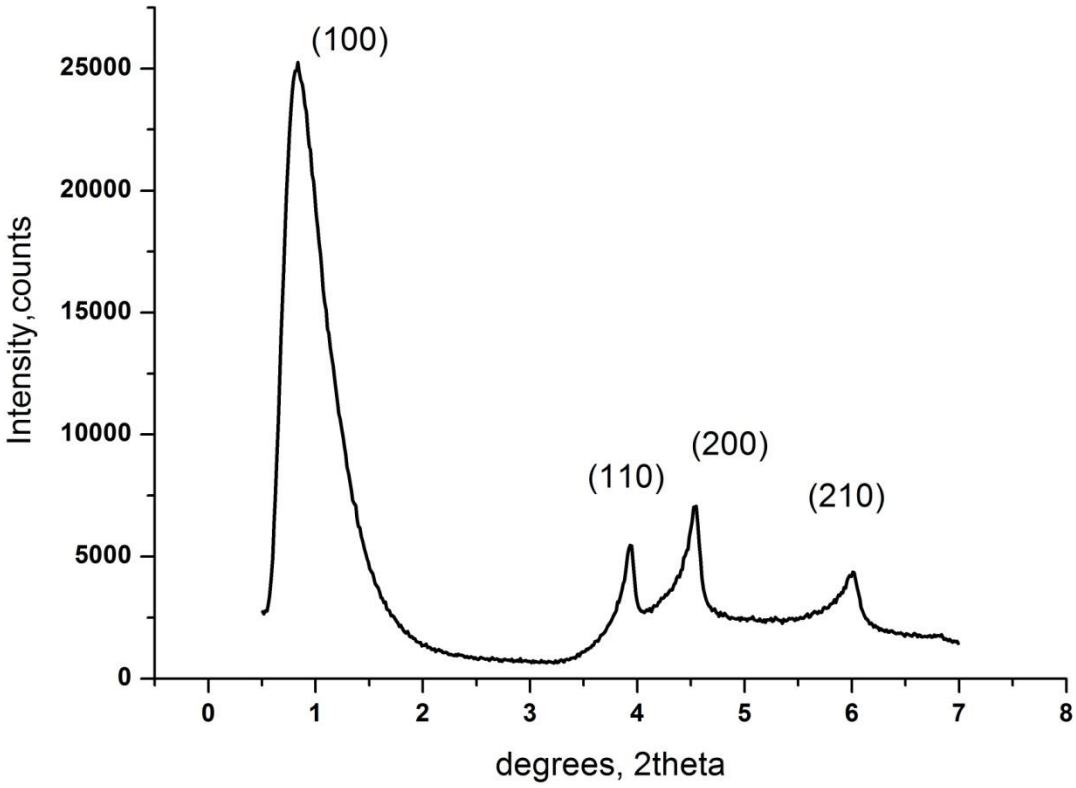

Figure. 21 X-ray diffractogram of MSN.

The diffractogram shows four different well-resolved reflections. This shows its lattice has hexagonal structure.

In addition to SEM characterization, size measurements were done by using ZetaSizer. The measurement was repeated three times. According to these measurements %26 of the particles has the highest number of particles have the size of 122 nm in aqueous media. The polydispersity index of the particles were 0.5. (Figure. 22)

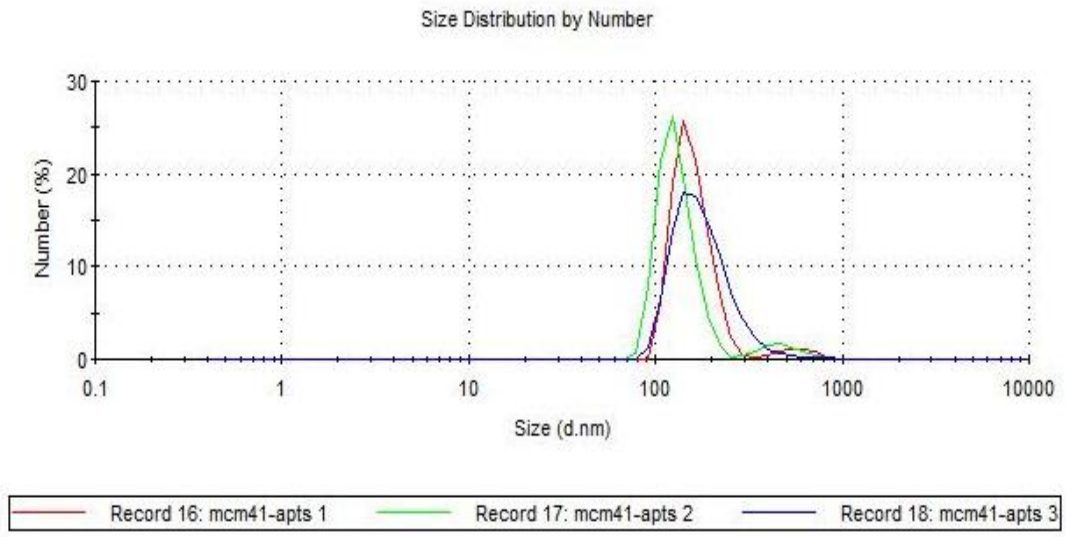

Figure. 22 Size distribution of MSNs in water.

Zeta potential measurements were obtained by using ZetaSizer. The zeta potential measurements of MSNs were obtained in water and repeated three times. As it can be seen in figure. 23 the mean value of potential is at 33 mV which is out of the range -30mV – 30mV. This indicates that the solvent in which MSNs were dispersed was not proper. As a result, water was not a proper solvent for MSNs, in time it would precipitate. (Figure. 23)

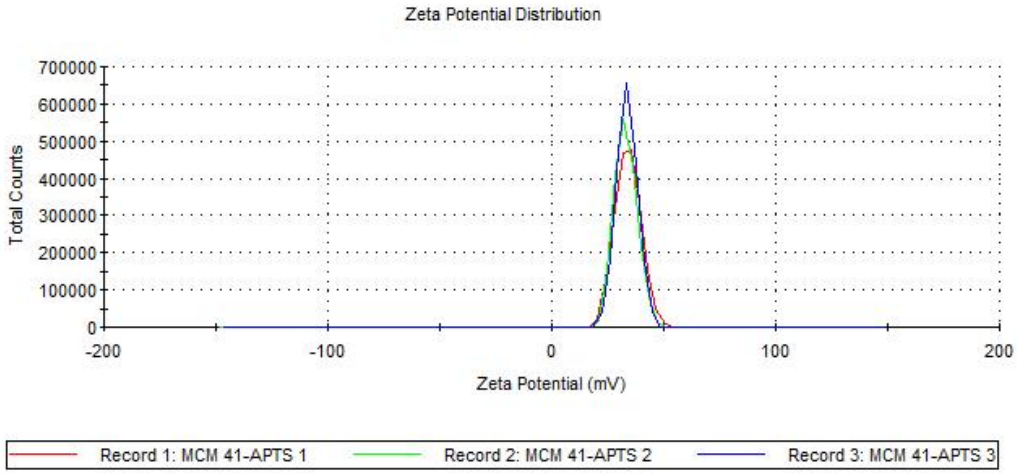

Figure. 23 Zeta potential distribution of MSNs

Nitrogen adsorption (physisorption) analysis characterizes the texturel properties of materials such as surface area, pore size, pore volume and pore geometry. The nitrogen isotherm of MCM-41 is shown in Figure 24. Both adsorption (black line) and desorption data (red line) are shown. As it can be seen in the graph, there are five districts. This isotherm is a typical MCM-41 isotherm. Accroding to BET analysis, the surface area of the particle is 1036 m^2/g, pore volume is 1.678 cc/g, pore size is 3.082 nm. The outgas temperature was 150^oC and the outgas time was 3 hours. (Figure 24)

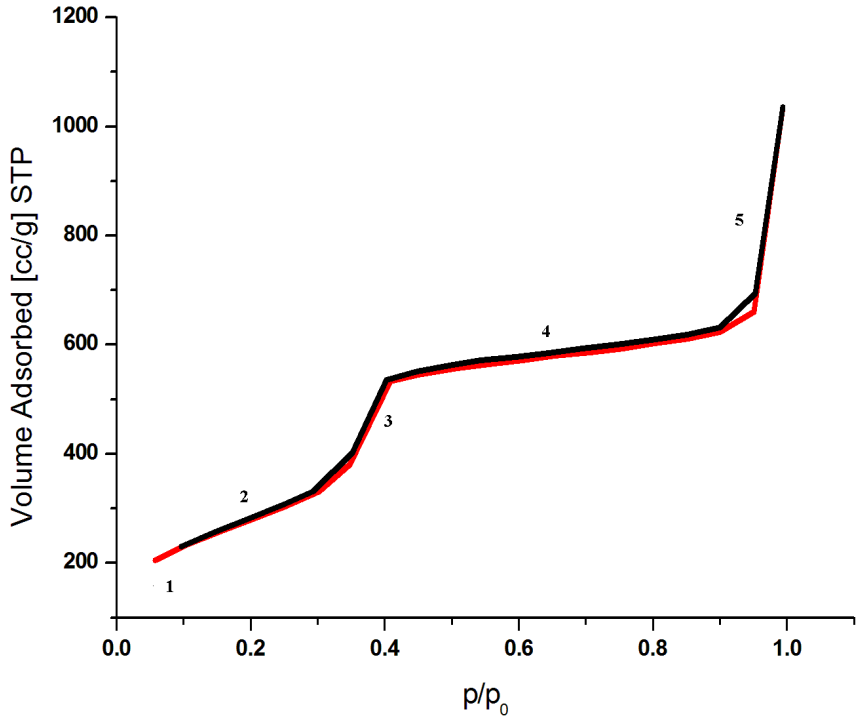

Figure 24. Nitrogen isotherm for all silica MCM-41.

Singlet oxygen generation capability of photosensitizer attached MSN (PS-MSNs) was measured by observing photobleaching of trap molecule 1,3-diphenylisobenzofuran (DPBF). $^1O_2$ species that are generated by excited photosenstizer react with DPBF and the decrease in absorbance value of DPBF was observed by using UV-Vis-NIR Spectrophotometer.

In order to observe singlet oxygen generation, we performed several number of experiments. First, the absorption of 0.67 mM DPBF solution was monitored after every 30 seconds of illumination by 660 nm LED light in every time. As shown in Figure. 24, there weren't observed any decrease in absorption peak of DPBF. This result indicates that photobleaching did not occur.

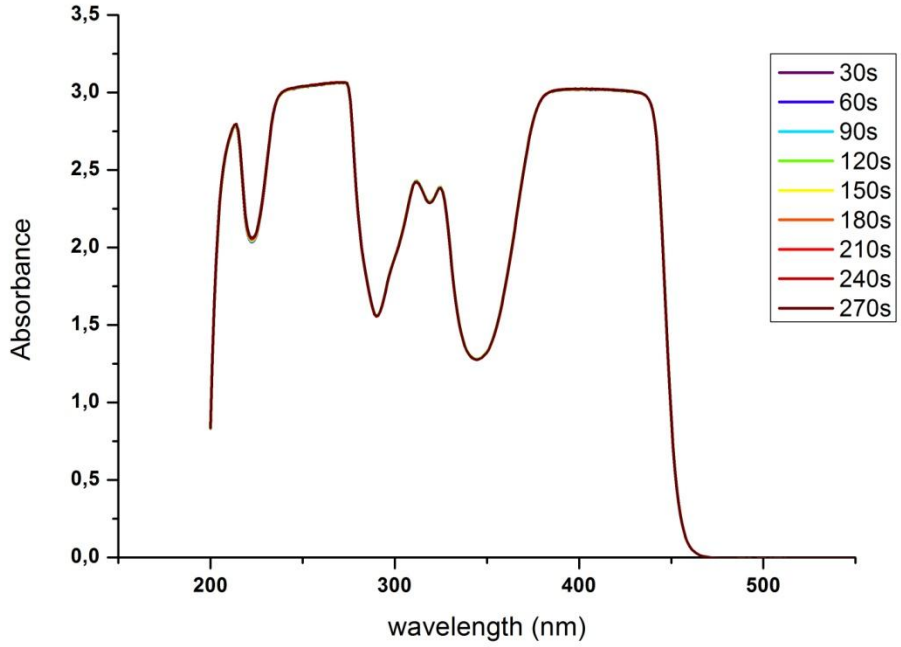

Figure. 25 Absorbance of DPBF in isopropanol. Each measurement was done after 30 seconds of illumination.

Second experiment was done in order to observe photobleaching of PS-MSNs. Measurements were done with 1 ml of PS-MSNs solution (8.2 mg PS-MSNs in 6 mL isopropanol) in 3 ml of isopropanol. The measurement was performed every time after 30 seconds of illumination as done with DPBF before. And the result shows that the rate of photobleaching is very low for PS-MSNs. (Figure. 25)

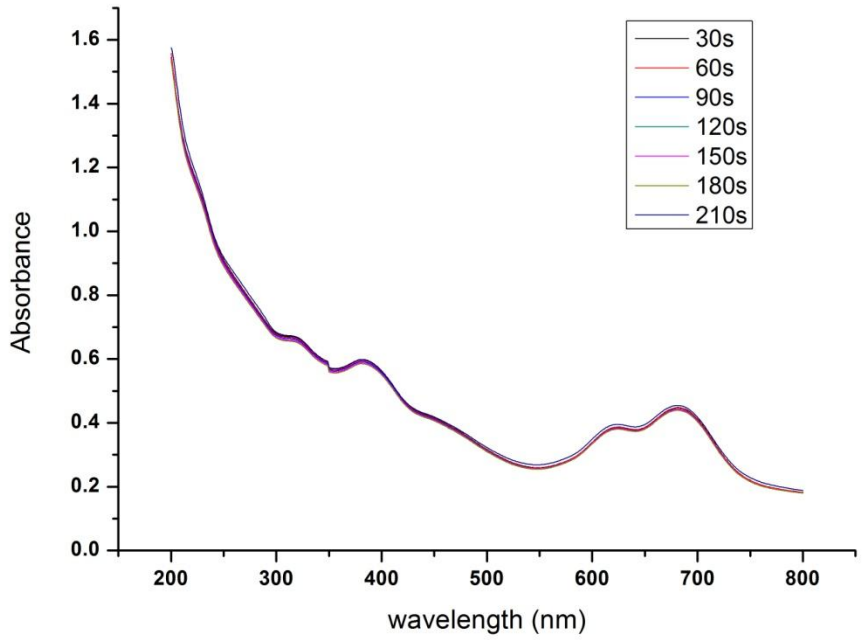

Figure 26. Absorbance spectra of PS-MSNs in isopropanol. Each measurement was done after 30 seconds of illumination.

Lastly, we performed the same measurement to observe singlet oxygen generation. 1ml PS-MSNs (8.2 mg PS-MSNs in 6 mL isopropanol), 0,5 ml DPBF (3 mM), 1.5 ml isopropanol was mixed together, 2 ml of the mixture was taken into 1 ml of isopropanol and the measurements were done. Each measurement was taken after illuminated 30 seconds by 660 nm LED light. As shown in Figure 27, there observed a decrease in absorbance in every time that the solution was illuminated. This indicates that the photosenstizer can generate singlet oxygen efficiently when illuminated under light of 660 nm.

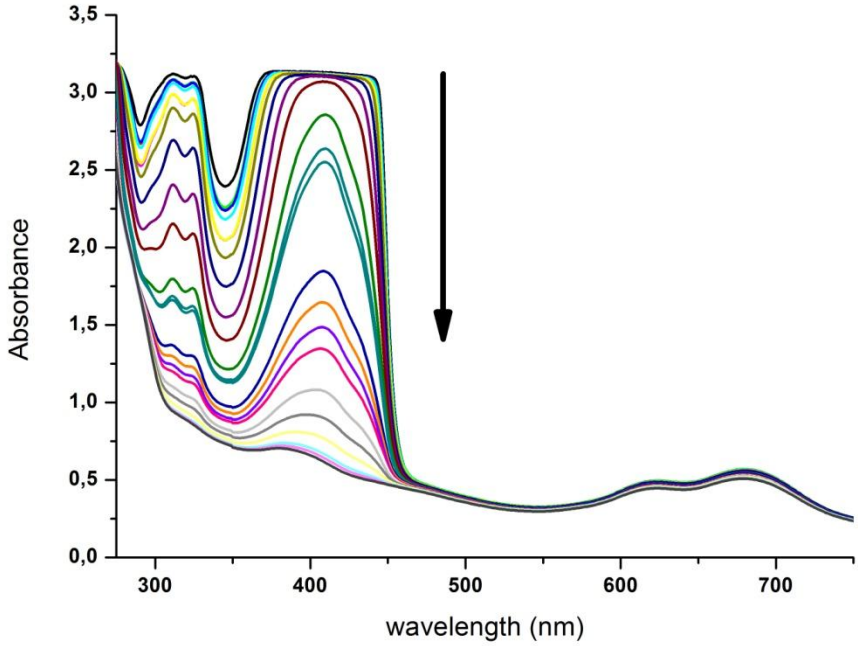

Figure 27. Bleaching of DPBF in the presence of PS-MSNs.

CHAPTER 4

CONCLUSION

In this study, novel BODIPY-based photodynamic therapy reagent and a carrier system were designed, synthesized and characterized. We studied to modify BODIPY dye to attach MSNs covalently. The photosenstizer has a 653 nm absorption maxima which makes it a good candidate to be used in PDT.

We synthesized MCM-41 type MSNs in order to use as drug carrier system. We used the instruments SEM, TEM, XRD, ZetaSizer in order to characterize MSNs. Since MSNs have amine groups on surface, it is easy to modify them in order to enhance targeting.

Singlet oxygen generation experiments show that the compound **9** is a good singlet oxygen generator and the carrier system does not influence the efficiency of singlet oxygen generation.

In conclusion, we have demonstrated that for PDT, MSNs can be used in the delivery of PS with the low toxicity, uniform pores, easily modified surface of MSNs and BODIPY dyes are good PSs with the efficent singlet oxygen generation.

REFERENCES

1. Weishaupt, K.R.; Gomer, C.J.; Dougherty, T.J; *Cancer Res.*, **1976**, *36*, 2326

2. Dougherty, T.J.; Gomer, C.J.; Henderson, B.W.; Jori, G.; Kessel, D.; Korbelik, M.; Moan, J.; Peng, Q.; *J. Natl. Cancer Inst.*, **1998**, *90*, 889

3. Detty, M.R.; Gibson, S.L.; Wagner, S.L.; *J. Med. Chem.*, **2004**, *47*, 3897

4. Henderson, B.W.; Dougherty, T.J.; *Photochem Photobiol*, **1992**, *55*, 145

5. Moan, J.; Berg, K.; *Photochem. Photobiol.*, **1991**, *53*, 549

6. Spikers, J.D. *Primary Progresses in Biology and Medicine.* Plenum Press, New York, **1985**, 209

7. Reed, M.; Ackroyd, R.; Kelty, C.; Brown, N.; *Photochem Photobiol*, **2001**, *74*, 656

8. Finsen, N.R.; *Phototherapy*, Edward Arnold, London, **1901.**

9. Fitzpatrick, T.B.; Pathak, M.A.; *J. Investig. Dermatol.*, **1959**, *23*, 229

10. Von Tappeiner, H.; Jesionek, A.; *Muench. Med. Wochenschr.* **1903**, *47*, 5

11. Von Tappeiner, H.; Jodlbauer, A.; *Gesammte Untersuchung uber die photodynamische Erscheinung*, F.C.W. Vogel, Leipzig, **1907.**

12. Hausmann, W. *Biochem.*, **1911**, *30*, 276.

13. Meyer-Betz, F., *Dtsch. Arch. Klin. Med*. **1913**, *112*, 476

14. Dougherty, T.J., *Cancer Res.*, **1978**, *36*, 2628

15. Kelly, J.F.; Snell, M.E., *J. Urol.*, **1976**, *115*, 150

16. Sandeman, D.R., *Lasers Med. Sci.*, **1986**, *1*, 163

17. Schweitzer, V.G., *Otolaryngol. Head Neck Surg.*, **1990,** *102*, 225

18. Barr, H.; Krasner, N.; Boulos, P.B.; Chatlani, P.; Bown, S.G., *Br. J. Surg*., **1990**, *77*, 93

19. Ward, B.G.; Forbes, I.J.; Cowled, P.A.; McEvoy, M.M.; Cox, L.W., *Am. J. Obstet. Gynecol.*, **1982**, *142*, 356

20. Triesscheijn, M.; Baas, P.; Schellens, J.H.M.; Stewart, F.A.; *The Oncologist*, **2006**, *11*, 1034

21. Gomer, C.J.; *Photodynamic Therapy, Methods in Molecular Biology*, Springer Science+Business Media, **2010**

22. Castano, A.P.; Mroz, P.; Hambli, M.R. *Nature Reviews Cancer,* **2006**, *6*, 535

23. Reed, M.W.; Wieman, T.J.; Schuschke, M.T.; Miller, F.N., *Radiot. Res.* , **1989**, *119*, 542.

24. Peng, Q.; Moan, J.; Nesland, J.M.; *Ultrastruc. Pathol.*, **1996**, *20*, 109.

25. Kessel, D.; Luo, Y., *J. Photochem. Photobiol.*, **1998**, *42*, 89.

26. Spikes, J.D.; Bommer, J.C. *Photochem. Photobiol.*, **1993**, *58*, 346.

27. Wang, R.K.; Tuchin, V.V., *Proc. SPIE*, **2003**, *4956*, 314

28. Brown, B.; Brown, E.A.; Walker, I., *Lancet Oncol.*, **2004**, *5*, 497

29. Gilson, D.; Ash, D.; Driver, I., *Br. J. Cancer*, **1988**, *58*, 665

30. Moriowaki, S.I.; Yoshinari, Y., *Photodermatol. Photoimmunol. Photomed.*, **2001**, *17*, 241

31. Loudet, A.; Burgess, K., *Chem. Rev.*, **2007**, *107*,4891

32. Karolin, J.; Johansson, L.B.A.; Strandberg, L.; Ny, T., *J. Am. Chem. Soc.* , **1994**, *116*, 7801

33. Metzker, M.L., WO Patent WO/2003/066812, **2003**

34. Ozlem S.; Akkaya E. U. *J. Am. Chem. Soc.*, **2009**, *131*, 48.

35. Yogo, T.; Urano, Y.; Ishitsuka, Y.; Maniwa, F.; Nagano, T. *J. Am. Chem. Soc.*, **2005**, *127*, 12162.

36. Atilgan, S.; Ekmekci, Z.; Dogan, A. L.; Guc, D.; Akkaya, E. U. *Chem. Commun*., **2006**, 4398.

37. Buyukcakir, O.; Bozdemir, A.O.; Kolemen,S.; Erbas, S.; Akkaya, E.U., *Org. Let.*, **2009**, *11*, 4644

38. Van Nostrum, C.F., *Adv. Drug Delivery Rev.* ,**2004**, *56*,9

39. Wang, S.; Gao, R.; Zhou, F.; Selke, M., *J. Mater. Chem.*, **2004**, *14*, 487.

40. Ohulchanskyy, T.Y.; Roy, I.; Goswami, L.N.; Chen, Y.; Bergey, E.J.; Pandey, R.K.; Oseroff, A.R.; Prasad, P.N., *Nano Lett.*, **2007**, *7*, 2835.

41. Zhang, P.; Steelant, W.; Kumar, M.; Scholfield, M., *J. Am. Chem. Soc.*, **2007**, *129*, 4526.

42. F. Iskandar, I.W. Lenggoro, T.O. Kim, N. Nakao, M. Shimada, K. Okuyama, *J. Chem. Eng. Jpn.*, **2001**, *34*, 1285.

43. Le Paige, M., France, US Patent, 3493341, **1970**

44. Yanagisawa, T.; Shimizu, T; Kuroda, K; Kato, C.; *Bull. Chem. Soc. Jpn.*, **1990**, *63*, 988

45. Kresge, C.T.; Leonowicz, M.E.; Roth, W.J.; Vartuli, J.C.; Beck, J.S.; *Nature*, **1992**, *359*, 710.

46. Kresge, C.T.; Leonowicz, M.E.; Roth, W.J.; Vartuli, J.C.; Beck, J.S.; Schmitt, K.D.; Chu, C.T-W.; Olson, D.H.; Sheppard, E.W.; McCullen, S. B.; Higgins, J.B.; Schlenker, J.L., *J. Am. Chem. Soc.*, **1992**, *114*, 10834.

47. Zhao. D., *Science*, **1998**, *279*, 548.

48. S.A. Johnson, P.J. Ollivier, T.E. Mallouk, *Science*, **1999,** *283*, 963.

49. Lensveld, D., *On the preparation and characterization of MCM-41 supported heterogeneous nickel and molybdenum catalysts*, Proefschrift Universitat Utrecht, **2003.**

50. Turro, N.J. In Modern Molecular Photochemistry; University Science Books; Sausalito, CA, **1991**, pp 191-195.

51. Wyszogrodzka, M.; Haag, R. *Chem. Eur. J.* ,**2008**, *14*, 9202.

52. Cheng, S.; Lee, C; Yang, C.; Tseng, F.; Mou, C.; Lo, L.; *J.Mater. Chem.;* **2009**, *19*, 1252.

APPENDİX A

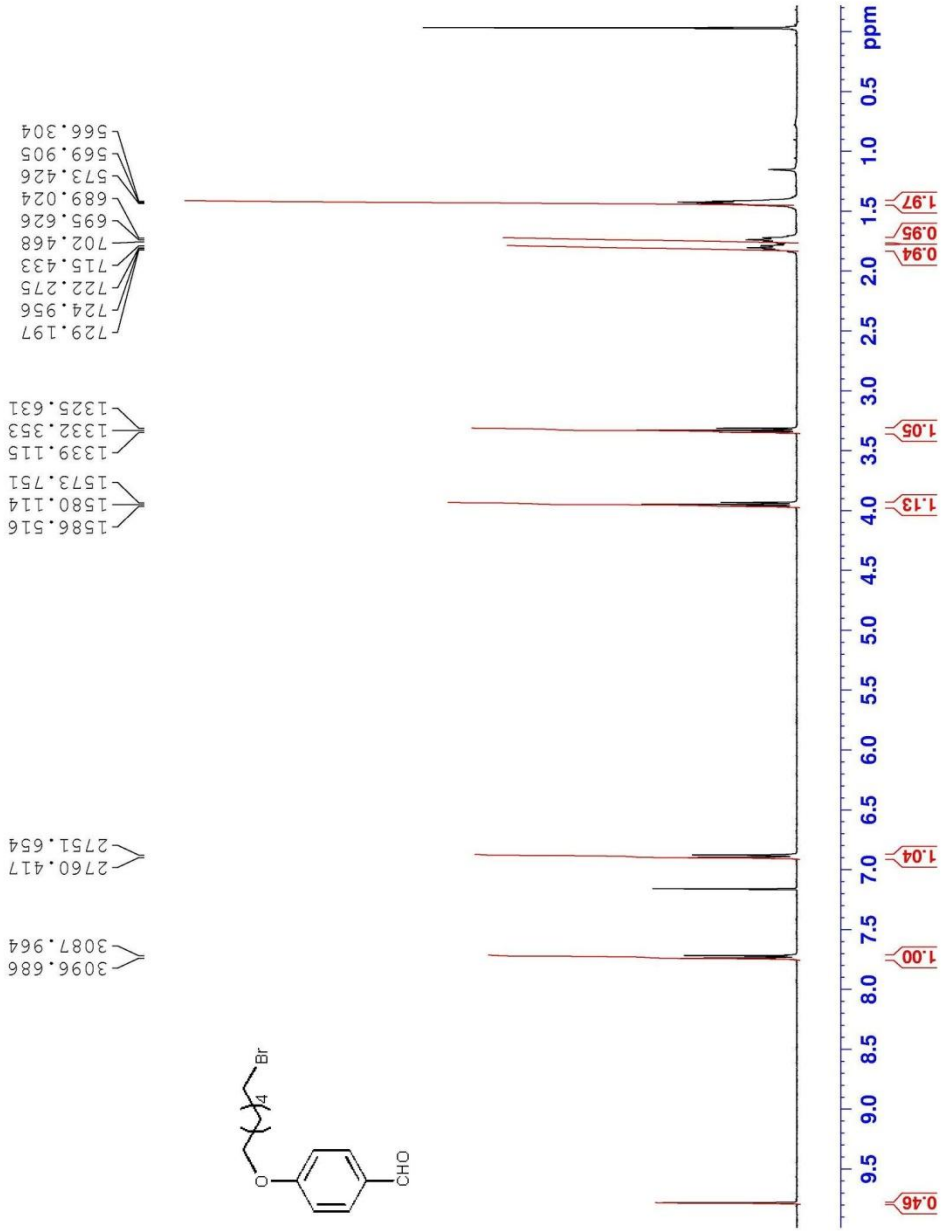

Figure 28. ^{1}H NMR of compound **3**

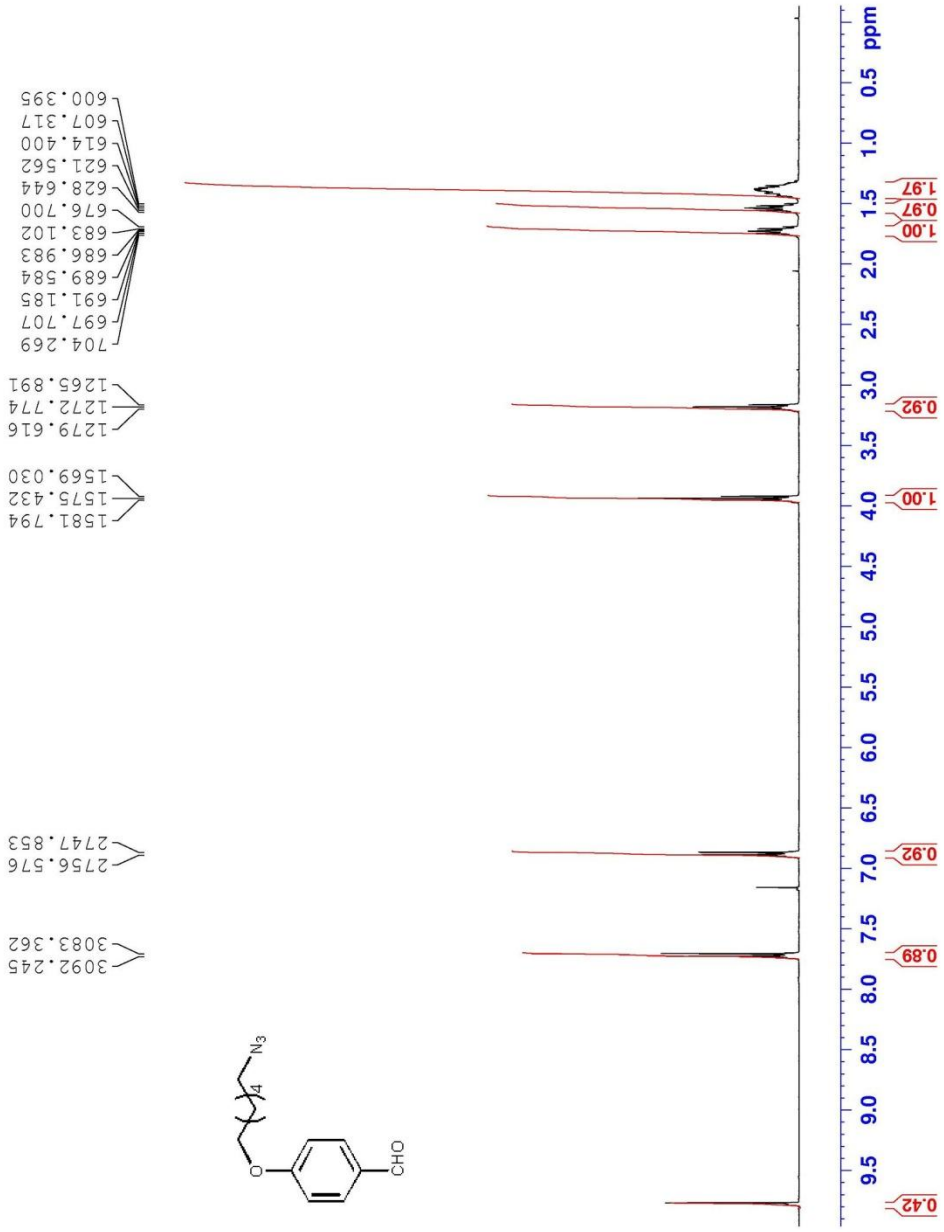

Figure 29. ^{1}H NMR of compound **4**

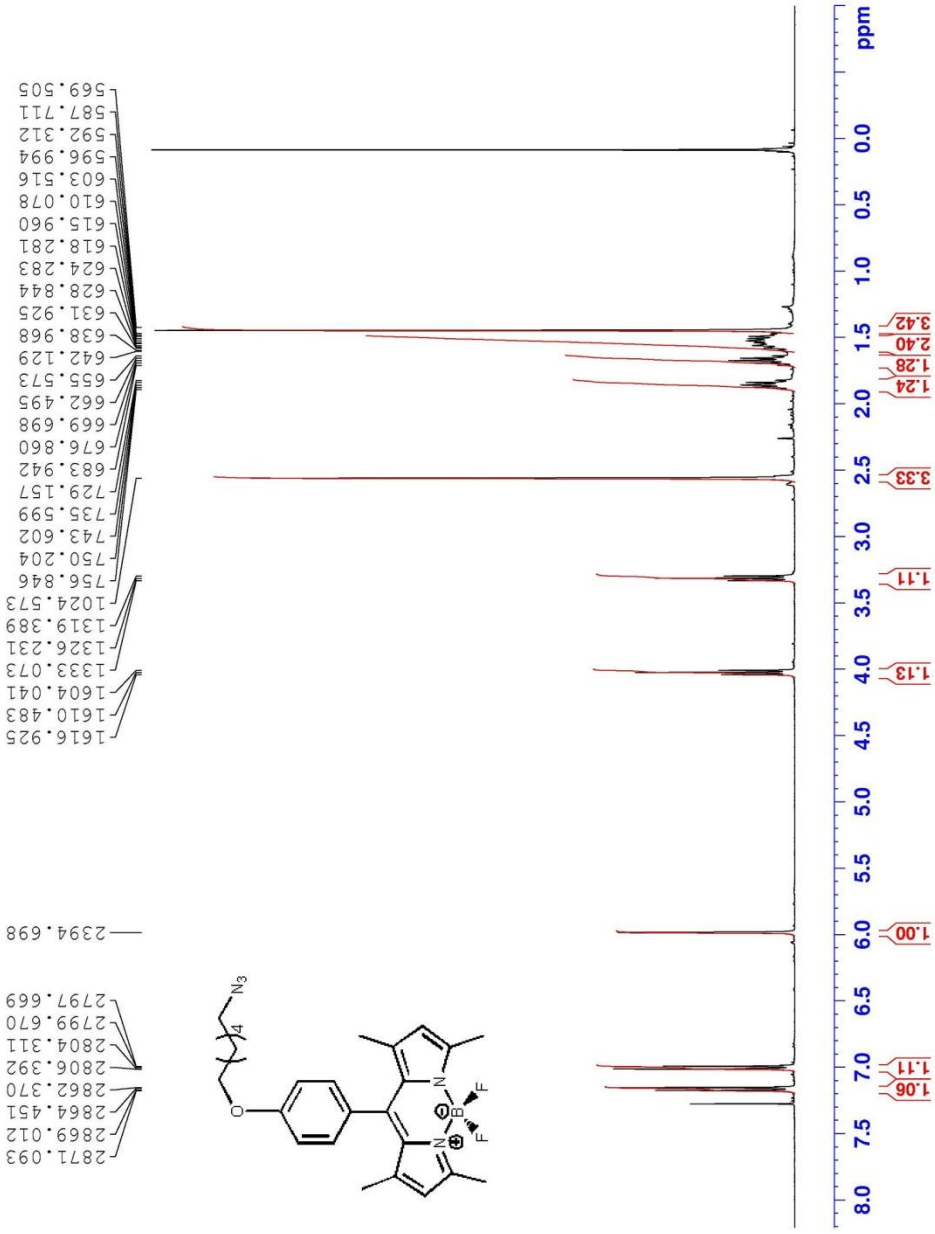

Figure 30. ^{1}H NMR of compound **5**

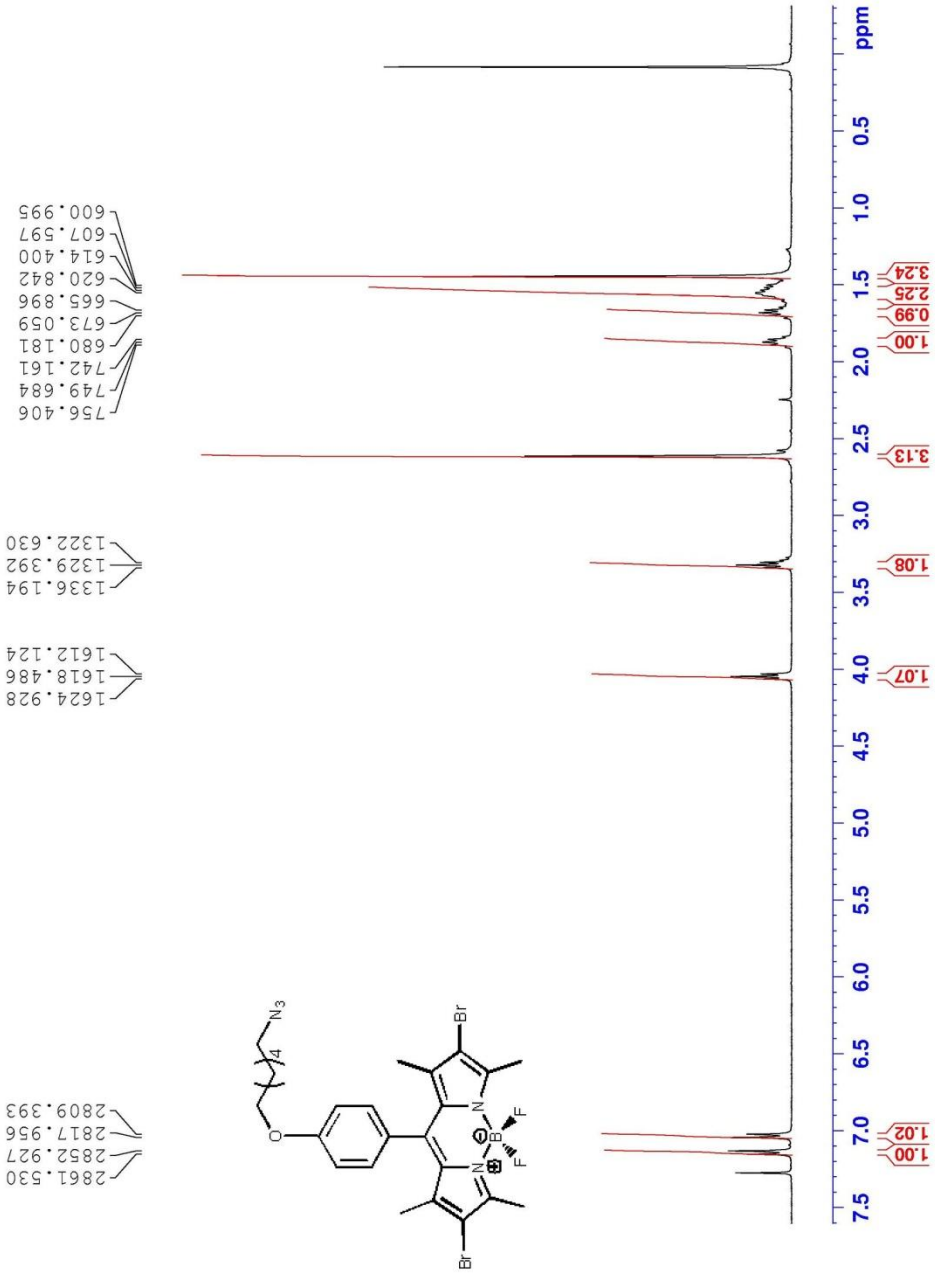

Figure 31. ^{1}H NMR of compound **6**

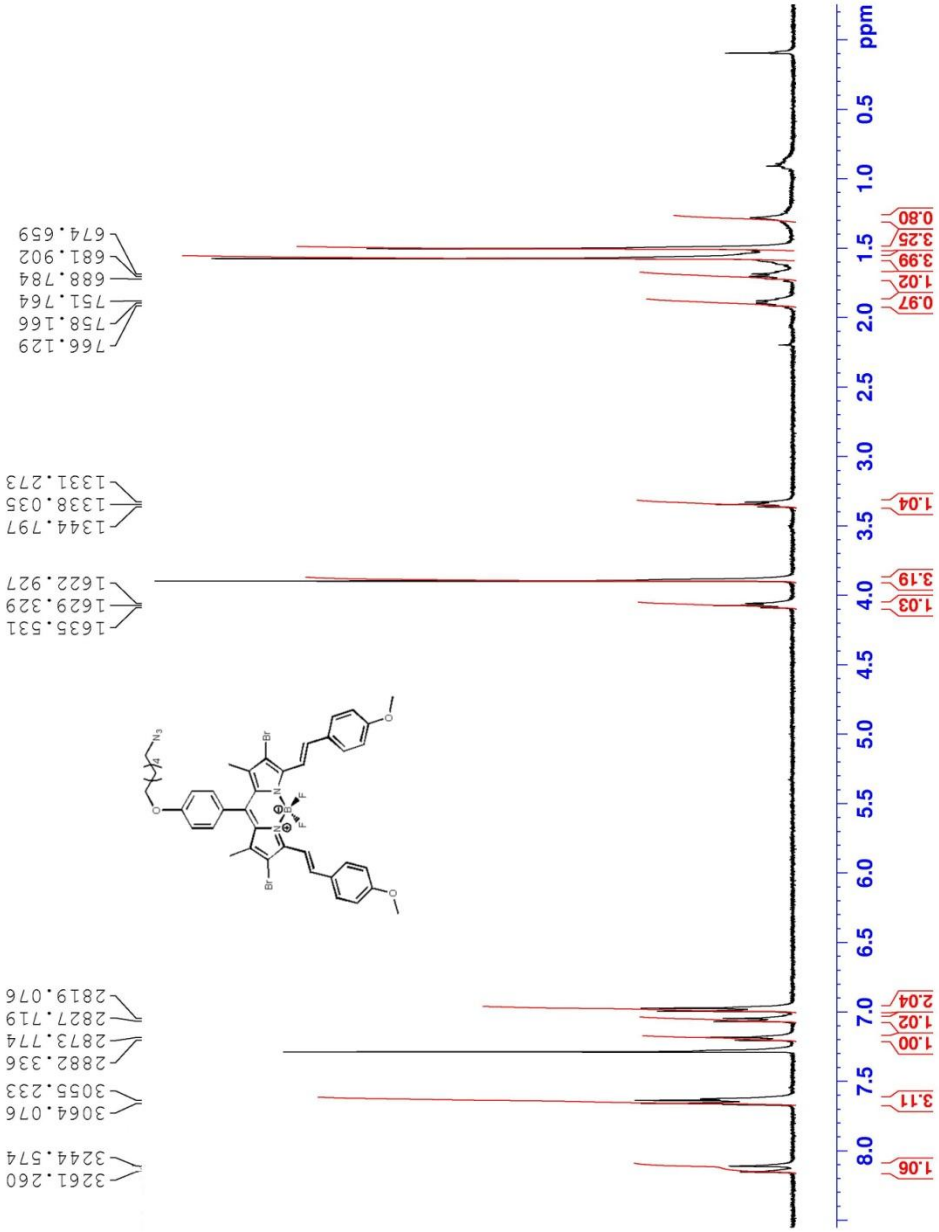

Figure 32. ^{1}H NMR of compound **7**

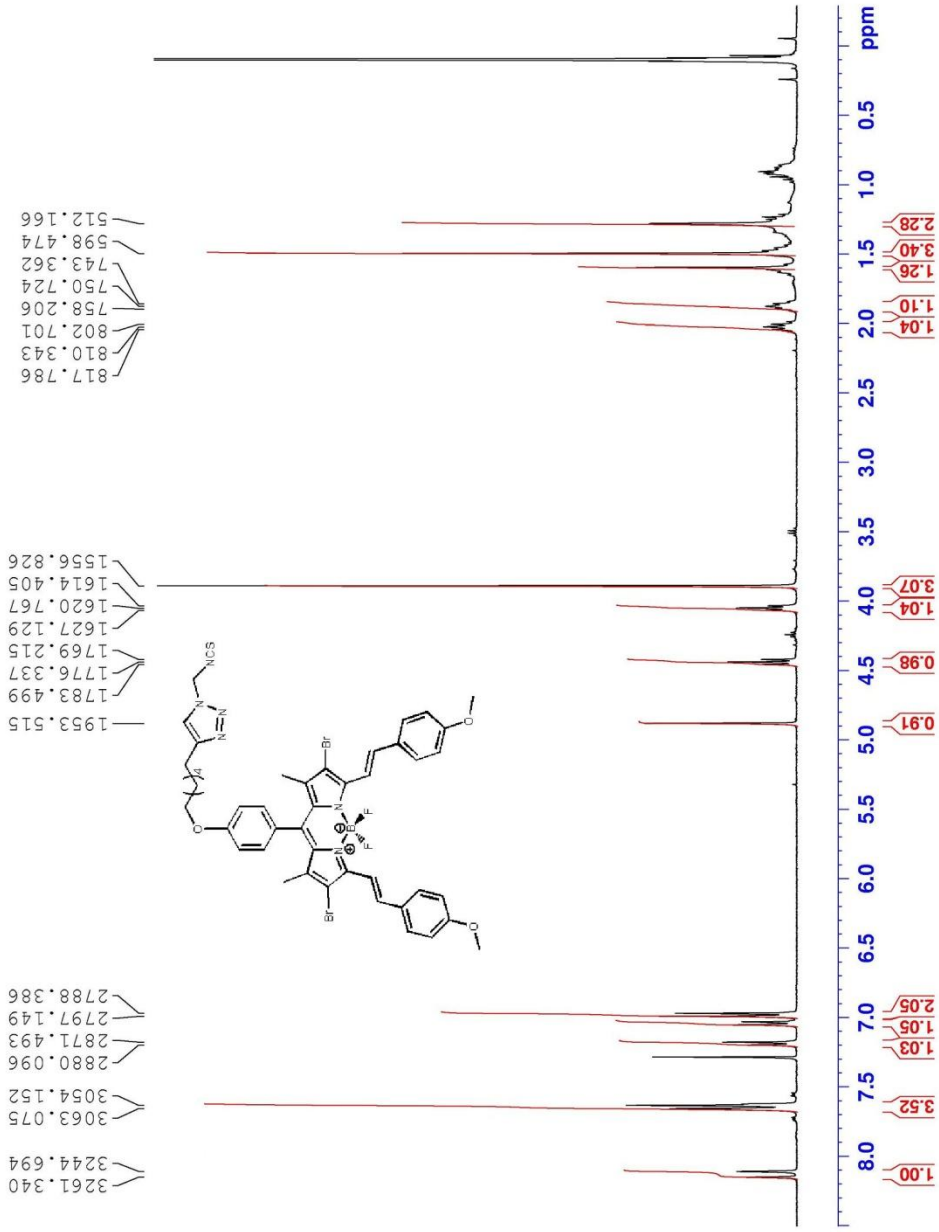

Figure 33. [1]H NMR of compound **9**

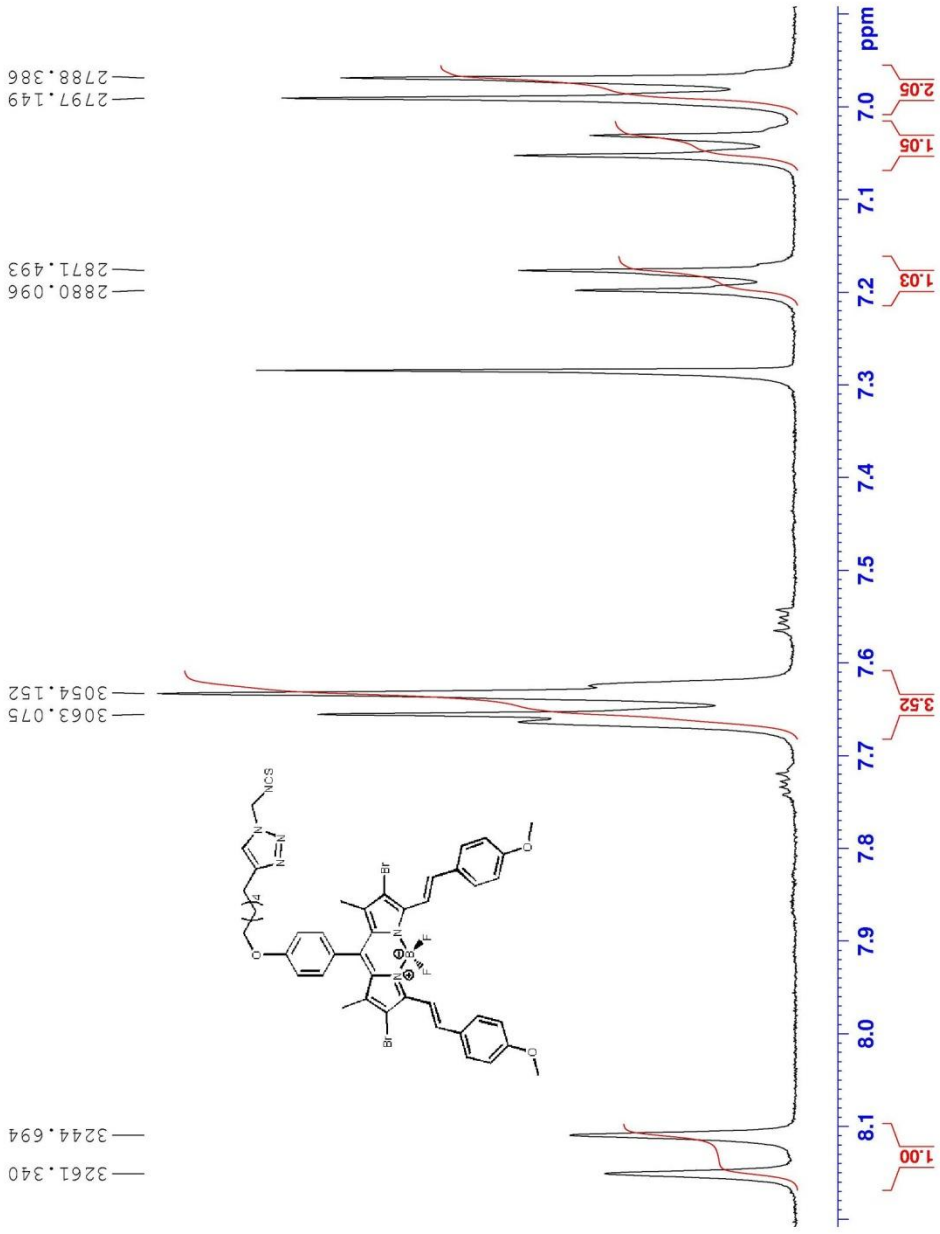

Figure 34. ^{1}H NMR of compound **9** (aromatic region)

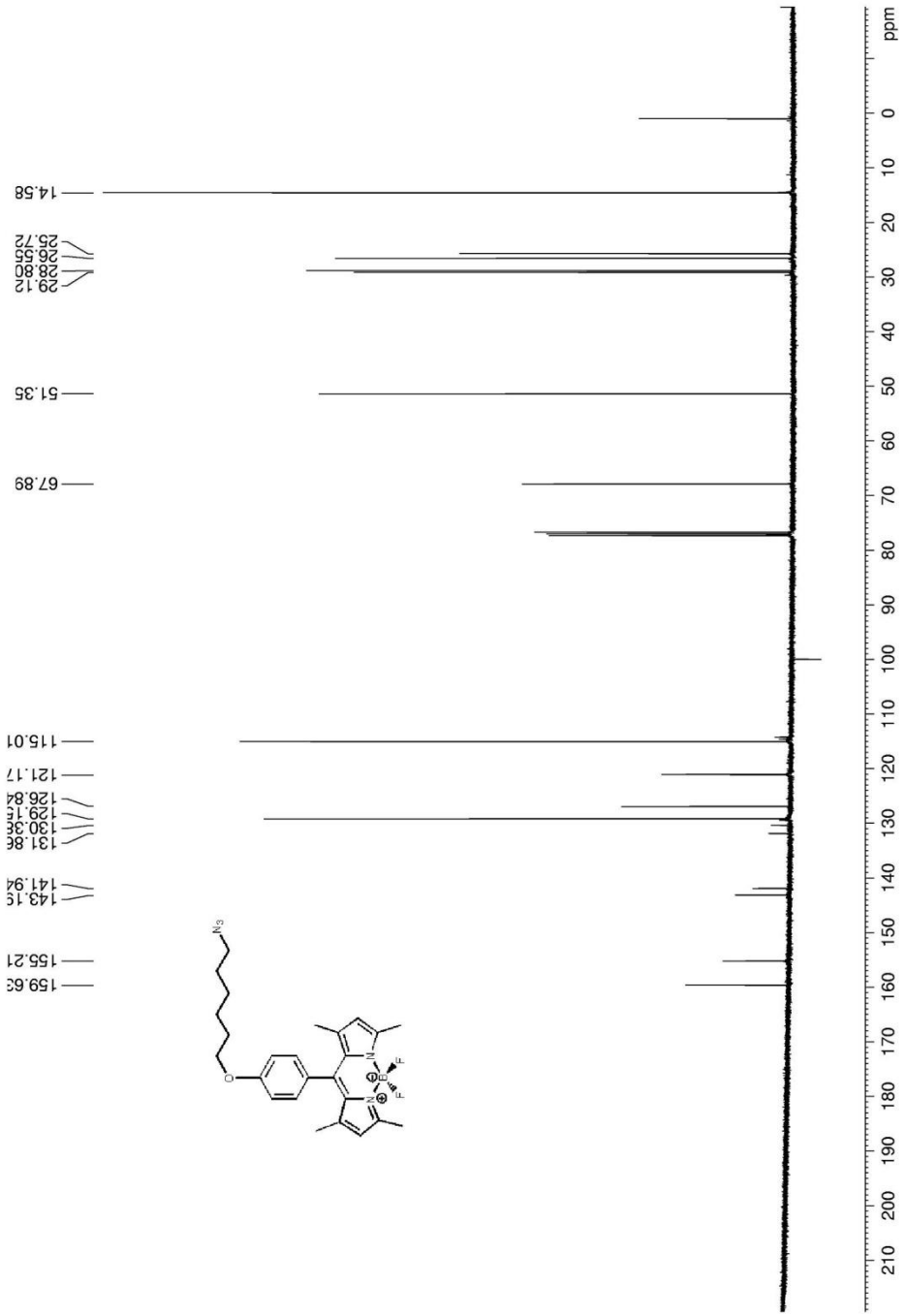

Figure 35. ^{13}C NMR of compound **5**

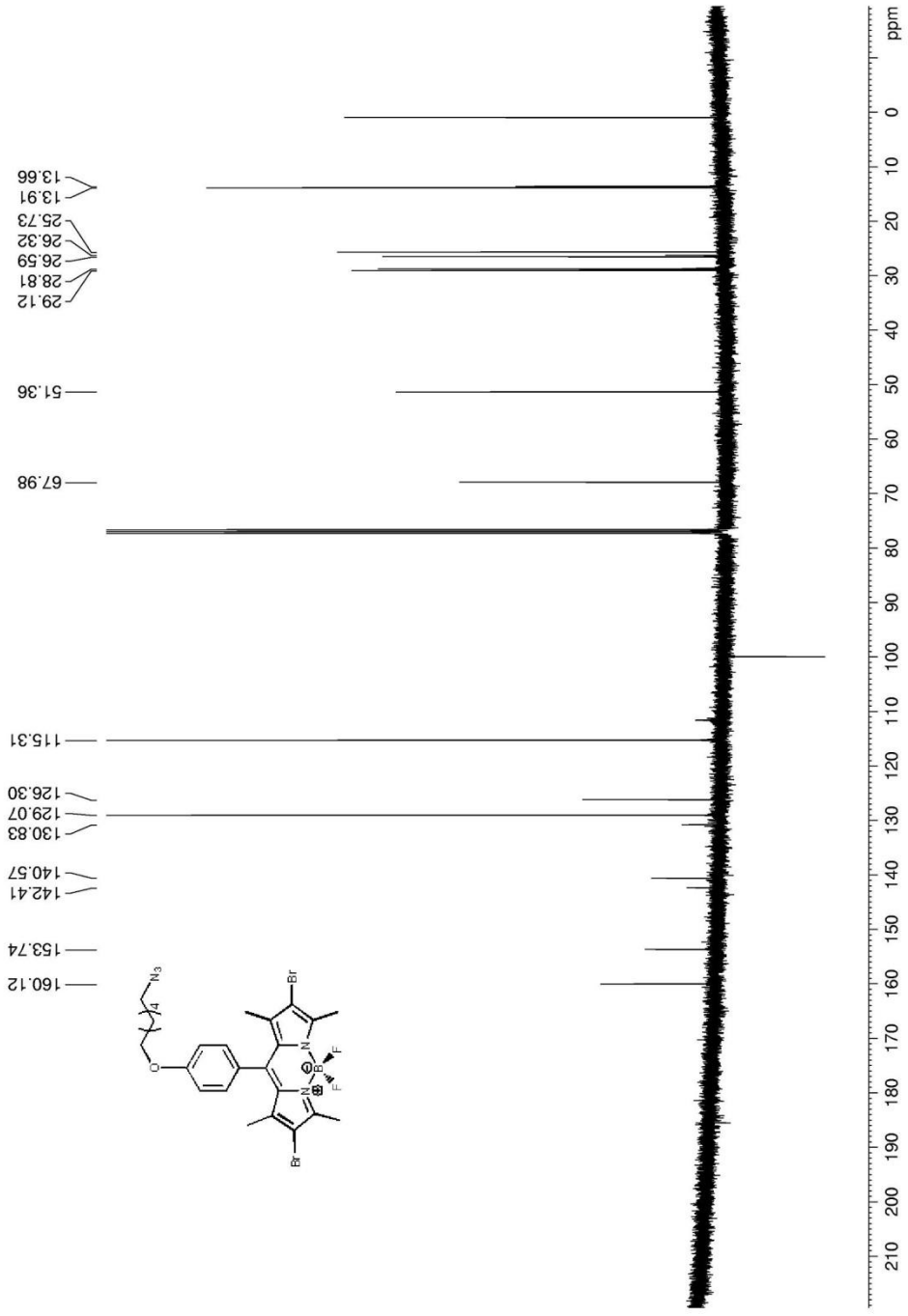

Figure 36. ^{13}C NMR of compound **6**

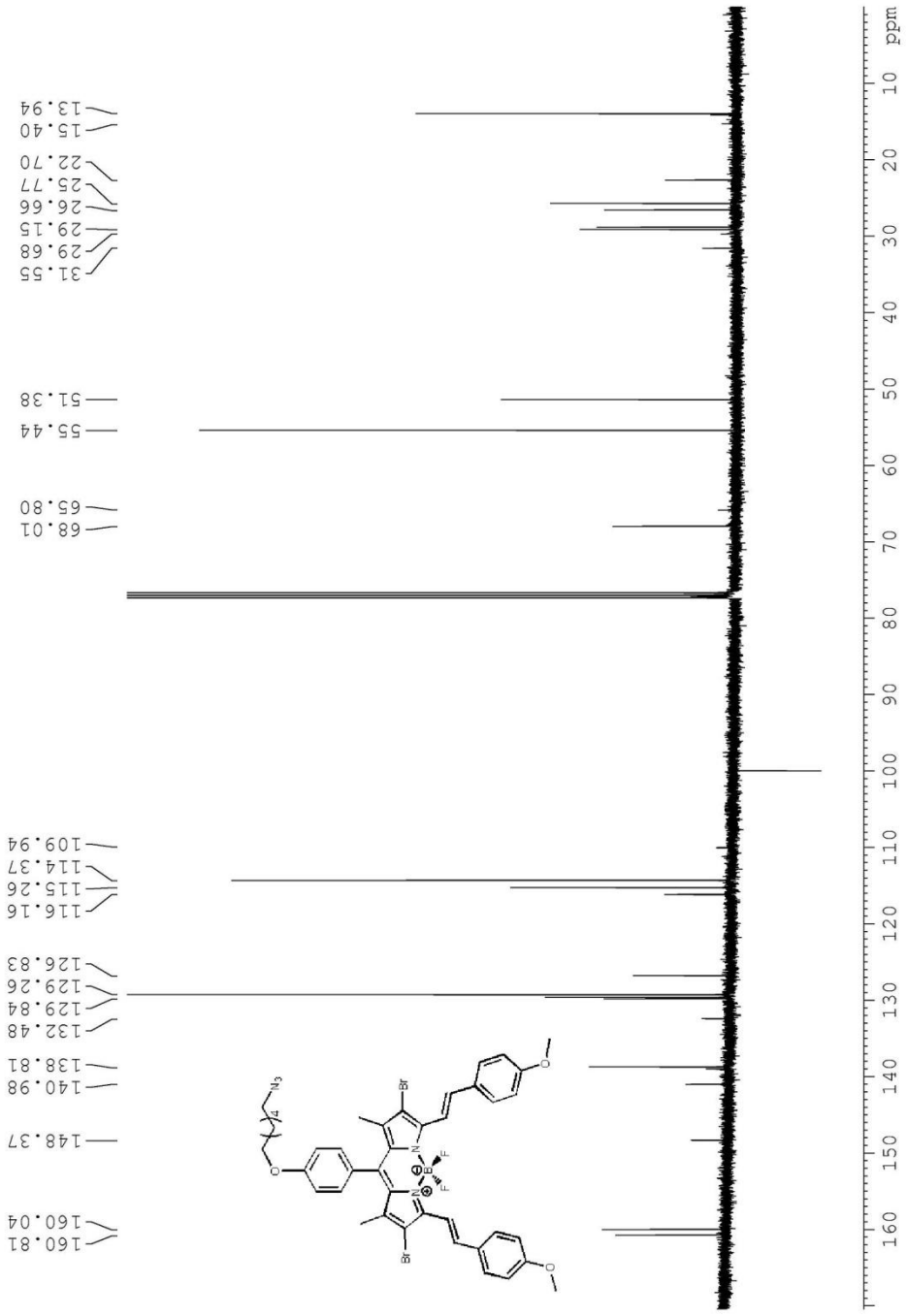

Figure 37. ^{13}C NMR of compound **7**

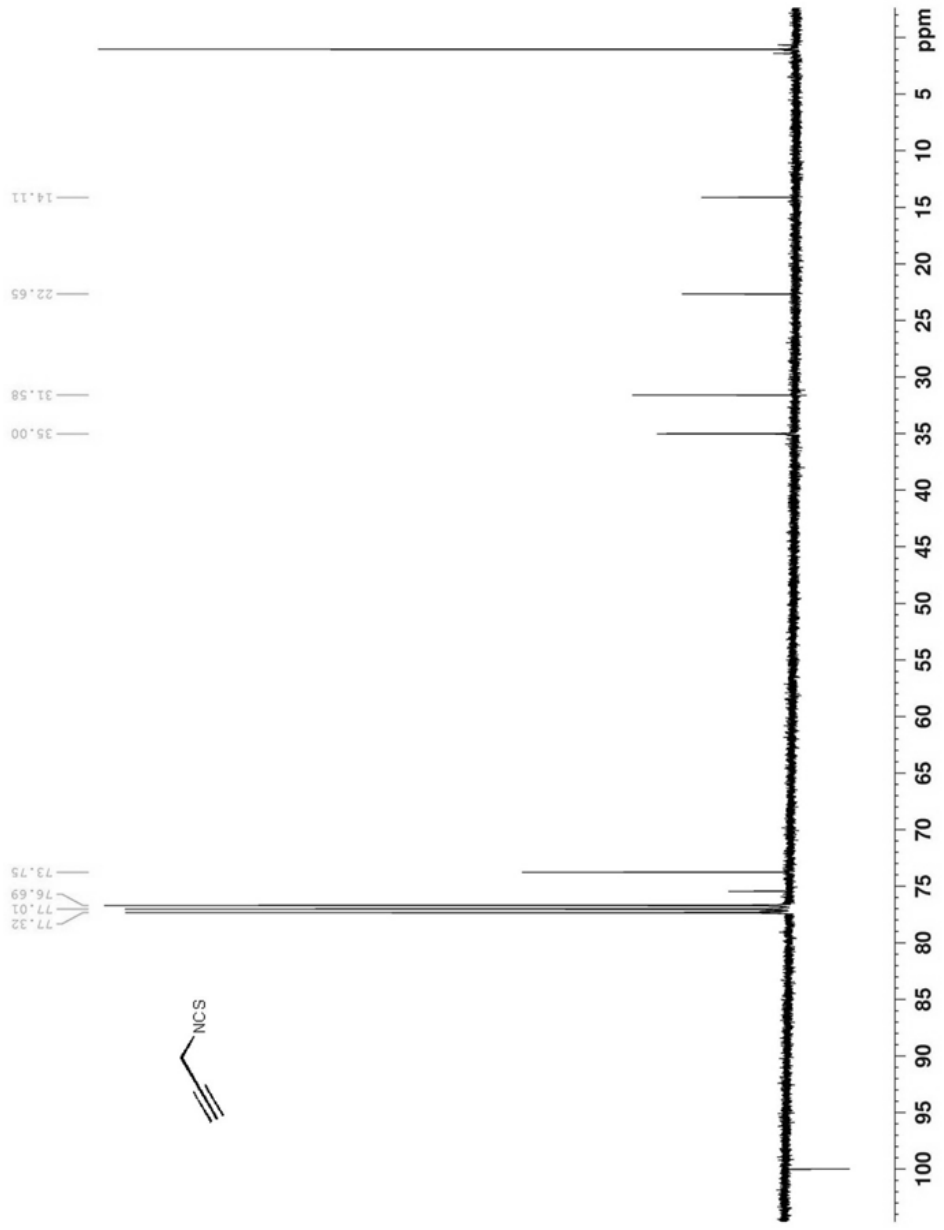

Figure 38. ^{13}C NMR of compound **8**

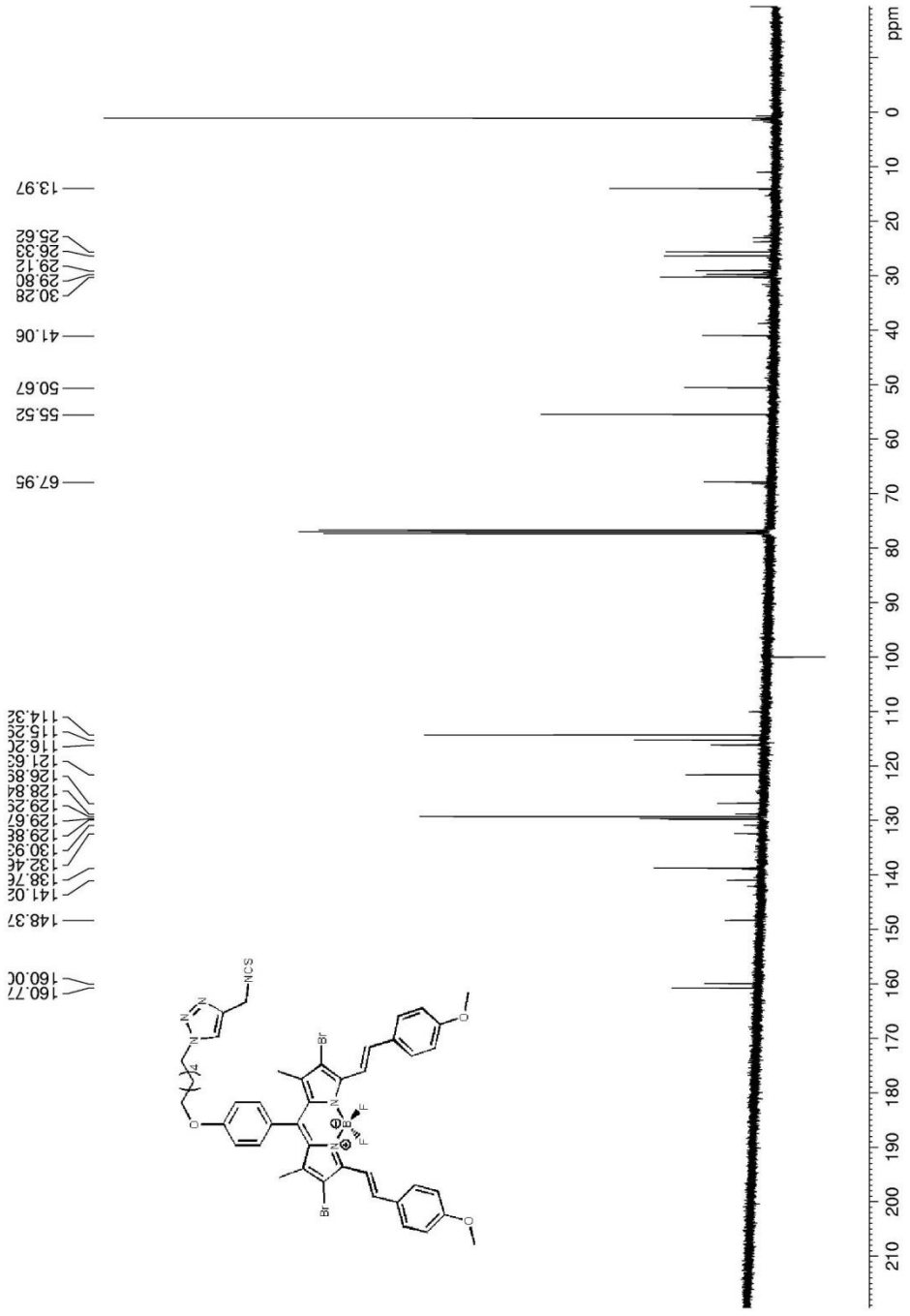

Figure 39. 13C NMR of compound 9

APPENDİX B

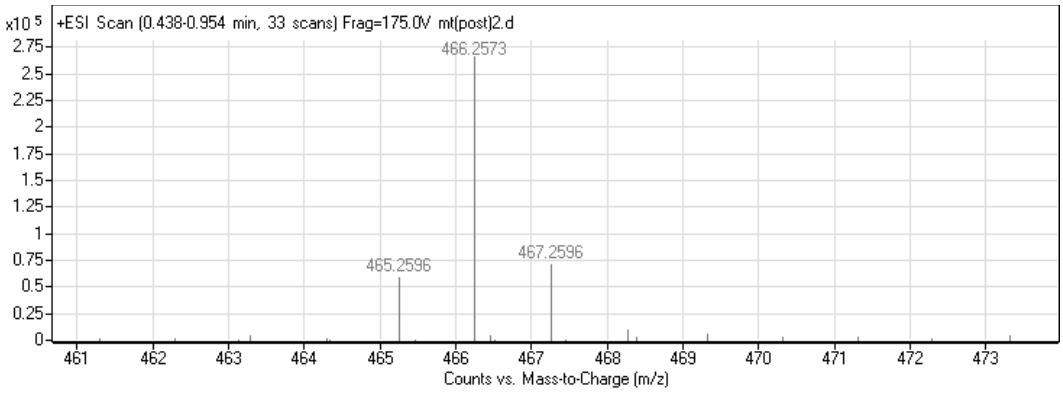

Figure 40. ESI-HRMS of compound **5**

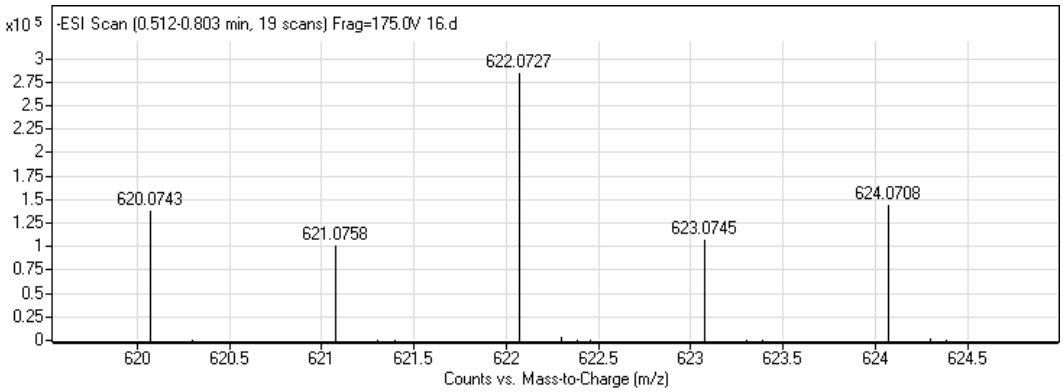

Figure 41. ESI-HRMS of compound **6**

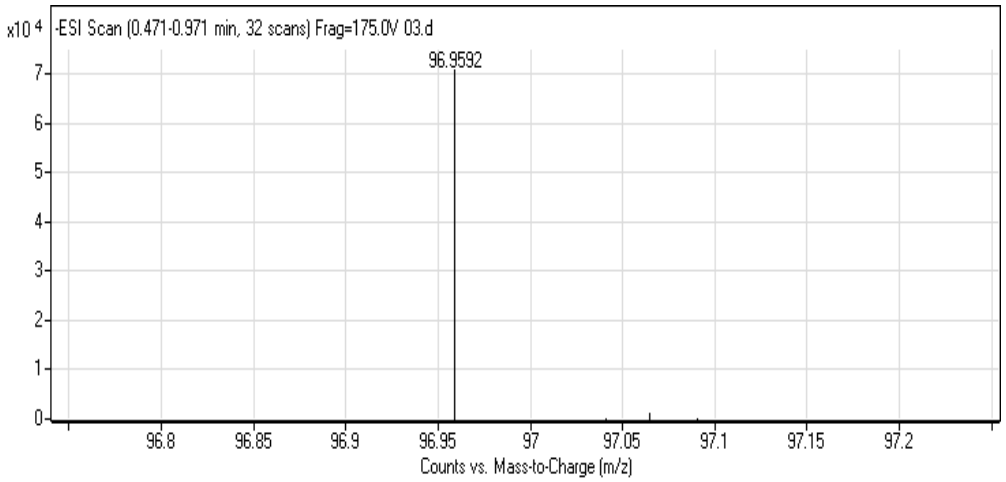

Figure 42. ESI-HRMS of compound **8**

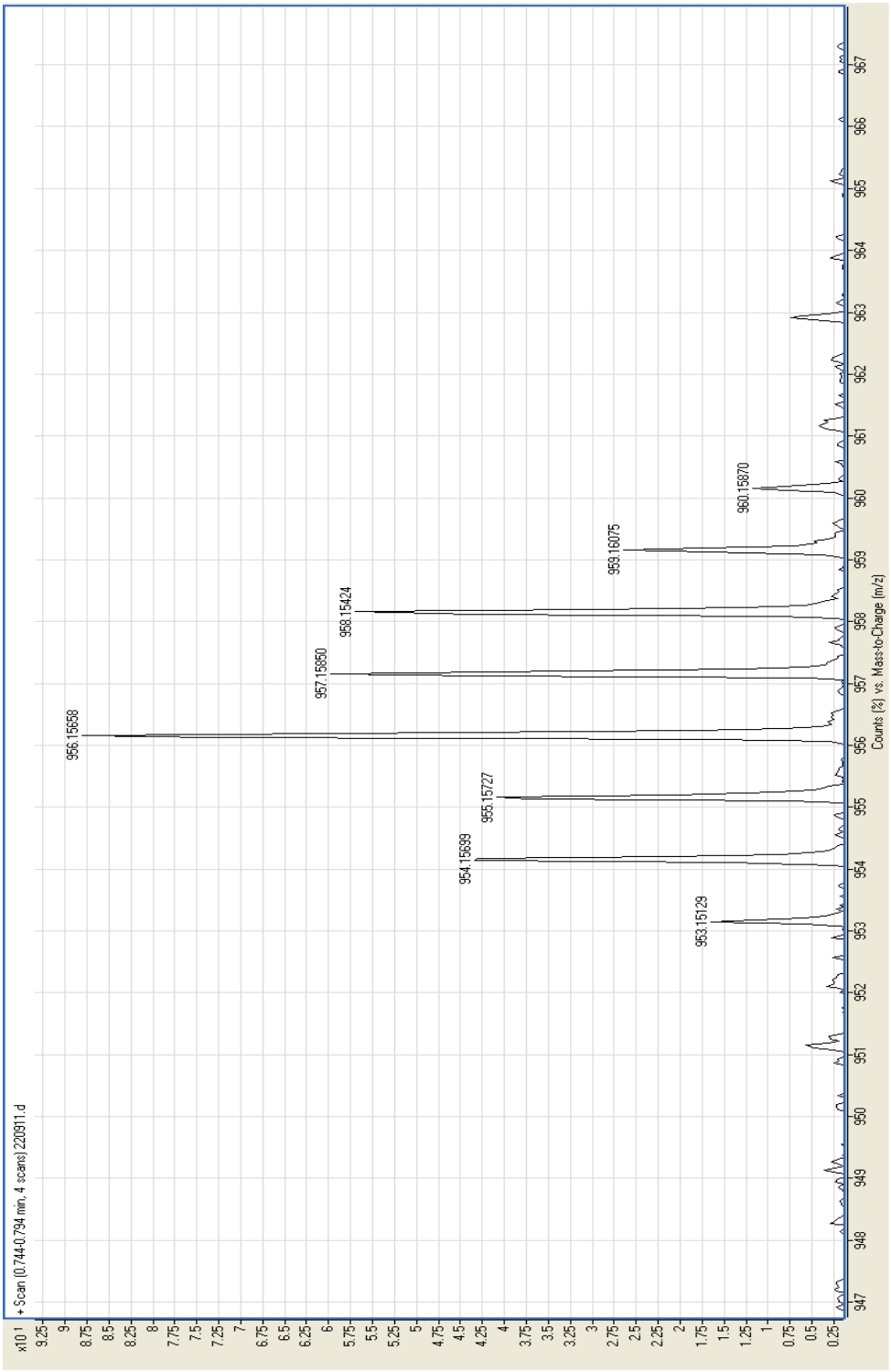

Figur 43. MALDI-MS of compound **9**